

Gravity Anomalies Seaward of Deep-Sea Trenches and their Tectonic Implications*

A. B. Watts and M. Talwani

(Received 1973 June 15)†

Summary

Studies of free-air gravity anomaly profiles across island arcs show an important belt of positive anomalies *seaward* of deep-sea trenches. This belt of positive anomalies is called the Outer Gravity High. The Outer Gravity High is well developed seaward of the central and eastern Aleutian, Kuril, Japan, northern Bonin and Philippine Trenches where it correlates with a regional rise in topography of a few hundred metres. The Outer Gravity High can be most satisfactorily explained by a stress system associated with the convergence of lithospheric plates at island arcs. The computed gravity effect of simple models of flexure of an oceanic plate approaching an island arc generally explain both the amplitude and wavelength of the Outer Gravity High. The Outer Gravity High seaward of the central and eastern Aleutian, Kuril, Japan, northern Bonin and Philippine Trenches can be explained by a horizontal compressive stress of the order of a few kilobars acting on the oceanic plate. The Outer Gravity High seaward of the southern Bonin and Mariana Trenches, however, can be explained in the absence of horizontal compressive stresses. These conclusions are consistent with differences in the stress field of island arcs as indicated by the seismicity and regional tectonics of the north-western Pacific. The Outer Gravity High is considered an important part of the regional gravity field of island arcs and the field derived from satellite observations. The close correlation of the Outer Gravity High with regional topography seaward of trenches suggest that the gravity effect of a dense downgoing slab beneath island arcs may be small and confined in lateral extent to the region of the island arc and trench. The prominent positive anomalies in island arc areas derived from satellite observations therefore owe a major part of their existence to causes other than the gravity effect of a dense downgoing slab.

Introduction

The concept of plate tectonics suggests that lithospheric plates diverge at mid-ocean ridges and converge at island arcs and deep-sea trenches (McKenzie & Parker 1967; Le Pichon 1968). The main tectonic elements of convergent plate boundaries are the island arc or orogen, the deep-sea trench and the trench-arc gap (Dickinson 1972). Recent studies indicate that marginal basins and coastal thrust belts landward

* Lamont-Doherty Geological Observatory Contribution No. 2029

† Received in original form 1973 April 4

of island arcs (Hasebe, Fuji & Uyeda 1970; Karig 1971a; Sleep & Toksöz 1971; Dickinson 1972) and outer rises in topography seaward of deep-sea trenches (Walcott 1970; Hanks 1971) are also important features of convergent plate boundaries.

Gravity surveys of convergent plate boundaries have usually been confined to the region of the island arc and deep-sea trench. The large amplitude positive anomalies of island arcs and negative anomalies of deep-sea trenches are well known from surveys using both pendulum apparatus (Vening Meinesz 1948; Worzel 1965) and surface-ship gravimeters (Talwani, Sutton & Worzel 1959; Talwani, Worzel & Ewing 1961; Hayes 1966). The gravity field of marginal basins landward of island arcs and the outer rise in topography seaward of deep-sea trenches are not, however, so well known.

In the past the gravity anomalies were usually interpreted in terms of crustal sections which are consistent with other geophysical data (Talwani *et al.* 1959; Peter, Elvers & Yellin 1965). Crustal sections are important because they give an idea of the mass distribution which can explain the gravity anomalies. However, they may not give an idea of the forces required to produce the anomalies. The gravity anomalies of convergent plate boundaries have recently been discussed in the framework of plate tectonics by Hatherton (1969, 1970) and Griggs (1972).

To examine some of these problems we have begun a study of gravity anomalies across convergent plate boundaries in the western Pacific. The study is based on selected profiles which extend sufficient distances to include the tectonic features of convergent plate boundaries both landward of island arcs and seaward of deep-sea trenches.

An important result of this study has been the delineation of a broad belt of positive gravity anomalies *seaward* of deep-sea trenches. We call this belt of positive anomalies the Outer Gravity High. The Outer Gravity High is up to 600 km wide and reaches amplitudes of +50 to +60 mgal. The Outer Gravity High trends subparallel to the adjacent deep-sea trench and is not present seaward of all trenches. The Outer Gravity High is well developed seaward of the central and eastern Aleutian, Kuril, Japan, northern Bonin and Philippine Trenches but is poorly developed seaward of the western Aleutian, southern Bonin and Mariana Trenches.

The purpose of this paper is to describe and interpret the Outer Gravity High. In addition, we attempt to evaluate the significance of the Outer Gravity High in relation to (1) the plate tectonic concept of the convergence of lithospheric plates at island arcs, (2) the seismicity and regional tectonics of island arcs, and (3) the regional gravity field of island arcs and the field derived from observations of satellites. We base this study primarily on recent data obtained on cruises of Lamont-Doherty vessels in the north-western Pacific.

Previous gravity surveys

Gravity measurements in the vicinity of island arcs and deep-sea trenches in the north-west Pacific have been obtained using both pendulum apparatus and surface-ship gravimeters. Surveys using pendulum apparatus have been described by Gainanov (1955) across the Sea of Okhotsk and Kuril Trench and by Worzel (1965) across the Bering Sea, Aleutian Trench, Japan Trench and the Bonin Trench. Surface-ship gravimeter surveys have been described for segments of the Aleutian Trench (Peter *et al.* 1965; Malahoff & Erickson 1969; Kienle 1971) and the Japan and Bonin Trenches (Tomoda, Segawa & Tokohiro 1970).

Gravity anomaly profiles across island arcs have been published by Gainanov (1955), Hayes & Ewing (1970), Segawa (1970) and Talwani (1970). In addition, land surveys of the Aleutian Arc (Woollard & Rose 1963; Barnes 1969; Carr *et al.* 1971) and the Japan Arc (Tomoda *et al.* 1970) have been published.

Data collection, reduction and presentation

This study utilizes gravity data obtained on Lamont-Doherty vessels *Vema* and *Robert D. Conrad* between 1964 and 1971. In addition, data obtained on cruises of *Pioneer* (U.S. Dept. of Commerce 1964) and *Umitaka-Maru* (Segawa 1970) have been used. The ship's tracks selected for study are shown in Fig. 1. A summary of the navigation and instrumentation used during individual cruises is given in Table 1.

In Table 1 the Gss 2 surface-ship gravimeters are the improved versions of the Graf-Askania gravimeters (Graf & Schulze 1961). Different platforms were utilized with the meter. The Anschutz platform with an oil erection system for erecting the gyroscope (Hayes, Worzel & Karnik 1964) is less accurate than later 'electrical erection' system where a short period pendulum and a filtering network is used. In the Alidade platform a U.S. Navy Mark IV Mod. 0 unit (using a short-period pendulum in a damped fluid as a vertical reference) is used to slave the platform. The Aeroflex platform also uses an 'electrical erection' system (Talwani 1970). The La Coste Romberg gravimeter is a gimbal mounted meter (La Coste & Harrison 1961) and the Japanese T.G.S.G. gravimeter is a vibrating string instrument (Tomoda & Kanamori 1962).

In addition to the measuring instrument used, the accuracy of the gravity data depends on a number of factors such as sea state, the cross-coupling correction and the accuracy of navigation. In general, we consider the measurements made on the electrically erected Anschutz and Aeroflex tables to be the most accurate. With satellite navigation and cross-coupling corrections the accuracy generally ranges from 2 to 5 mgal. On the other hand, with the Alidade platform with no cross-coupling and with celestial navigation the accuracy is in the range from 5 to 20 mgal.

Gravity data has been reduced to free-air gravity anomalies referred to the equilibrium figure of the Earth (flattening $1/299.8$). The equilibrium figure has been chosen because departures from it are indicative of hydrostatic stresses existing in the Earth, especially in the lithosphere. The resulting gravity anomalies are not, therefore, conventional anomalies which are referred to the international ellipsoid (flattening $1/297.0$). Gravity anomalies referred to the equilibrium figure can be converted to anomalies referred to the international ellipsoid for latitudes 0° , 20° N, 40° N and 60° N (Fig. 1) by adding +8, +6, -2 and -13 mgal respectively.

Gravity data are presented as a summary map (Fig. 1) and as projected profiles along ship's tracks (Figs 2-5). The Outer Gravity High discussed in the text is outlined in Fig. 1 and selected profiles across the feature are presented in Figs 2-5. A more detailed gravity anomaly map of the north-western Pacific contoured at 25-mgal interval is at present in preparation.

Topography data are presented as projected profiles along ship's tracks (Figs 2-5). Topography data seaward of the trench have been reduced to an arbitrary base-line at an estimated depth of the 'undisturbed' sea floor.

Description of the gravity anomaly profiles

Topography and free air anomaly profiles are presented along selected ship's tracks across the Aleutian, Kuril, Japan, Bonin and Mariana Trenches (Fig. 1) in Figs 2-4. In addition, profiles are presented across the Philippine and Ryukyu Trenches and the Nankai Trough in Fig. 5. The profiles have been projected approximately perpendicular to the trend of the trenches.

Aleutian Trench

Topography and free-air anomaly profiles of the Aleutian Trench between longitude 174° E and 150° W are presented in Fig. 2.

Profiles 1, 2 and 3 (Figs 1 and 2) cross the eastern Aleutian Trench and the smooth sea floor of the Aleutian abyssal plain south of Kodiak Island. The depth of the

Table 1
Instrumentation and data collection

Ship	Year	Cruise & leg	Profile Numbers (Figs 1-5)	Navigation	Gravimeter identification	Stable platform	Cross-coupling correction applied?	Comments
<i>Conrad</i>	1966	1007	17	Celestial	Gss2-6	Anschutz oil erection	No	
<i>Conrad</i>	1966	1010	4	Celestial	Gss2-6	Anschutz oil erection	No	
<i>Conrad</i>	1967	1107	26	Satellite	Gss2-6	Anschutz oil erection	Yes	
<i>Conrad</i>	1967	1108	7	Satellite	Gss2-6	Anschutz oil erection	Yes	
<i>Conrad</i>	1967	1109	1, 3, 5	Satellite	Gss2-6	Anschutz oil erection	Yes	
<i>Conrad</i>	1968	1206	34, 33	Satellite	Gss2-31	Anschutz electric erection	Yes	
<i>Conrad</i>	1968	1207	14	Satellite	Gss2-31	Anschutz electric erection	Yes	
<i>Conrad</i>	1968	1209	2	Satellite	Gss2-31	Anschutz electric erection	Yes	
<i>Conrad</i>	1969	1217	30	Satellite	Gss2-31	Anschutz electric erection	Yes	
<i>Conrad</i>	1969	1219	6, 15	Satellite	Gss2-31	Anschutz electric erection	Yes	
<i>Conrad</i>	1971	1405	9, 10, 11, 12, 13, 14, 16	Satellite	Gss2-31	Anschutz electric erection	Yes	
<i>Vema</i>	1963	1907	27, 24	Celestial	Gss2-12	Alidade with Mark IV Mod. 0 as vertical reference	No	

<i>Vema</i>	1964	2006	8	Celestial	Gss2-12	Alidade with Mark IV Mod. 0 as vertical reference	No	
<i>Vema</i>	1964	2008	32, 25	Celestial	Gss2-12	Alidade with Mark IV Mod. 0 as vertical reference	No	
<i>Vema</i>	1965	2106	18	Celestial	Gss2-12	Alidade with Mark IV Mod. 0 as vertical reference	No	Leg corrected by 10 mgal
<i>Vema</i>	1965	2107	31, 20	Celestial	Gss2-12	Alidade with Mark IV Mod. 0 as vertical reference	No	
<i>Vema</i>	1965	2108	28	Celestial	Gss2-12	Alidade with Mark IV Mod. 0 as vertical reference	No	
<i>Vema</i>	1965	2110	19	Celestial	Gss2-12	Alidade with Mark IV Mod. 0 as vertical reference	No	
<i>Vema</i>	1967	2405	29, 22	Satellite	Gss2-12	Lamont platform Mark IV Mod. 0 as vertical reference	Yes	
<i>Vema</i>	1971	2814	20	Satellite	Gss2-12	Aeroflex	Yes	
<i>Pioneer</i>	1964	Leg B	21	Celestial	LaCoste-Romberg air-sea gravimeter-S-11	Gimbal suspension	No	U.S. Dept. Commerce, (1969)
<i>Unitaka-Maru</i>	1968	Leg 12	23	Celestial	T.S.S.G. vibrating string	Vertical gyroscope	No	Segawa (1970)

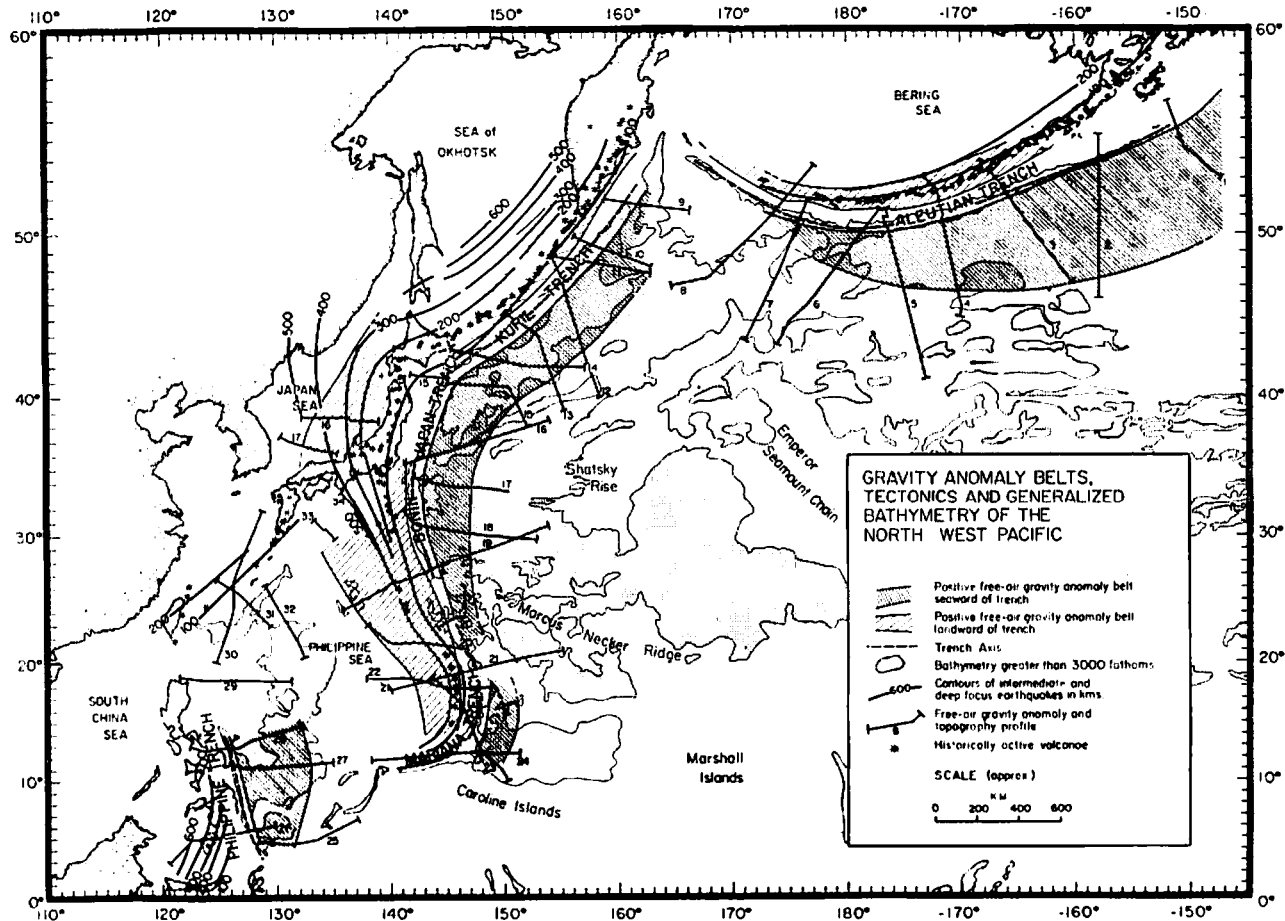


FIG. 1. Ship's tracks of *Vema*, *Robert D. Conrad*, *Pioneer* and *Umitaka-Maru* in the north-western Pacific selected in this study. Generalized bathymetry is based on Chase *et al.* (1970) and volcanoes based on the International Atlas of Active Volcanoes. Seismic contours were obtained from well determined intermediate and deep focus earthquakes and are shown at 100-km interval. The extent of the positive free-air gravity anomaly belts landward and seaward of trenches are indicated by diagonal shading. Note that the positive anomalies are widest seaward of the central and eastern Aleutian Trench and narrowest seaward of the Mariana Trench.

ALEUTIAN TRENCH

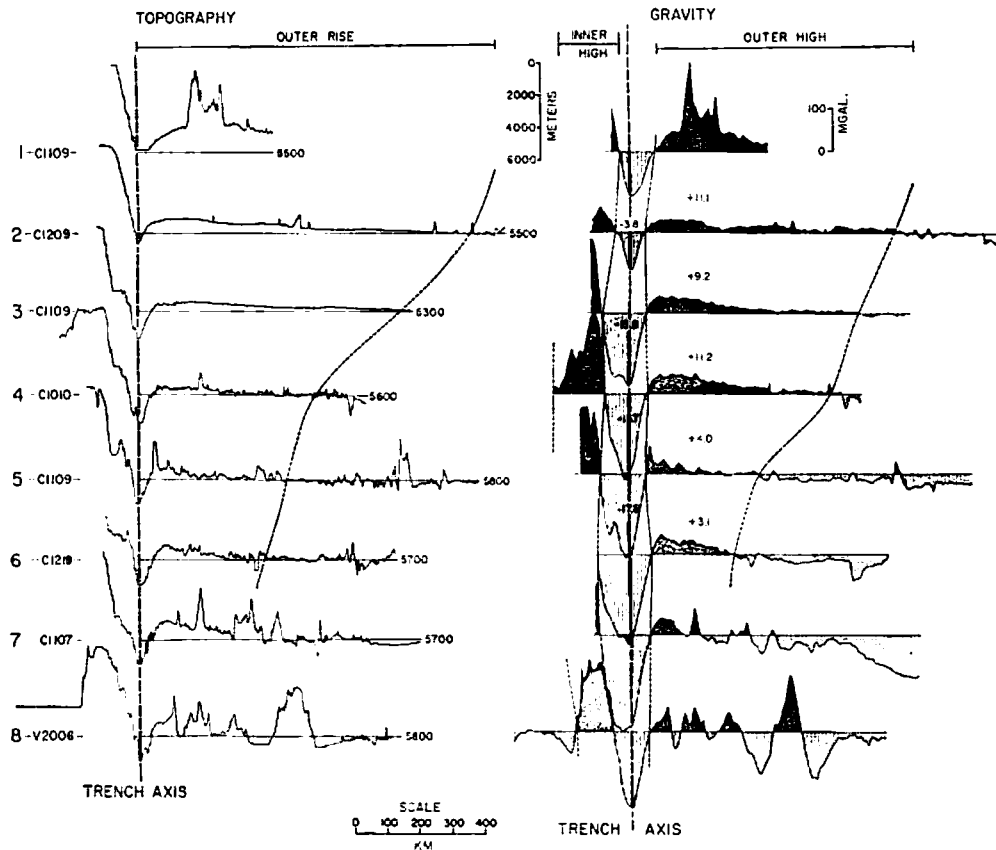


FIG. 2. Topography and free-air gravity anomaly profiles 1-8 (Fig. 1) of the Aleutian trench. The gravity anomalies have been referred to the equilibrium figure of the Earth (flattening $1/299.8$). Annotations above the gravity anomaly profiles indicate the integral of the profiles in units $\times 10^3$ mgal km between the segments of the profiles outlined by dashed lines. The profiles show an excellent correlation between a regional rise in topography of a few hundred metres seaward of the trench and positive gravity anomalies. The positive anomalies reach amplitudes up to $+55$ mgal and widths of 600 km seaward of the eastern Aleutian Trench.

trench increases from 5.3 km for profile 1 to 7.1 km for profile 3. The landward wall of the trench is steep (about 6°) on profiles 1 and 2 but is interrupted by a narrow bench at a depth of about 4.1 km on profile 3. The seaward wall of the trench is also relatively steep (about 3°). Seaward of the trench the profiles show a well developed regional rise in topography. The regional rise has also been noted by Mammerickx (1970) and correlates with seismic reflection profile evidence (Jones, Ewing & Truchan 1971) of a regional rise in the acoustic basement seaward of the trench. The amplitude of the regional rise estimated from mean depths of the 'undisturbed' sea floor north of the Surveyor Fracture Zone, is about 700 m.

Profiles 4, 5 and 6 cross the central and western Aleutian Trench and the irregular sea floor south of Adak Island. Profile 4 extends across the Aleutian Arc and the Aleutian Basin. The depth of the trench on profiles 4, 5 and 6 is about 7.3 km. The landward wall of the trench is characterized by a continuation of the narrow bench

KURIL TRENCH

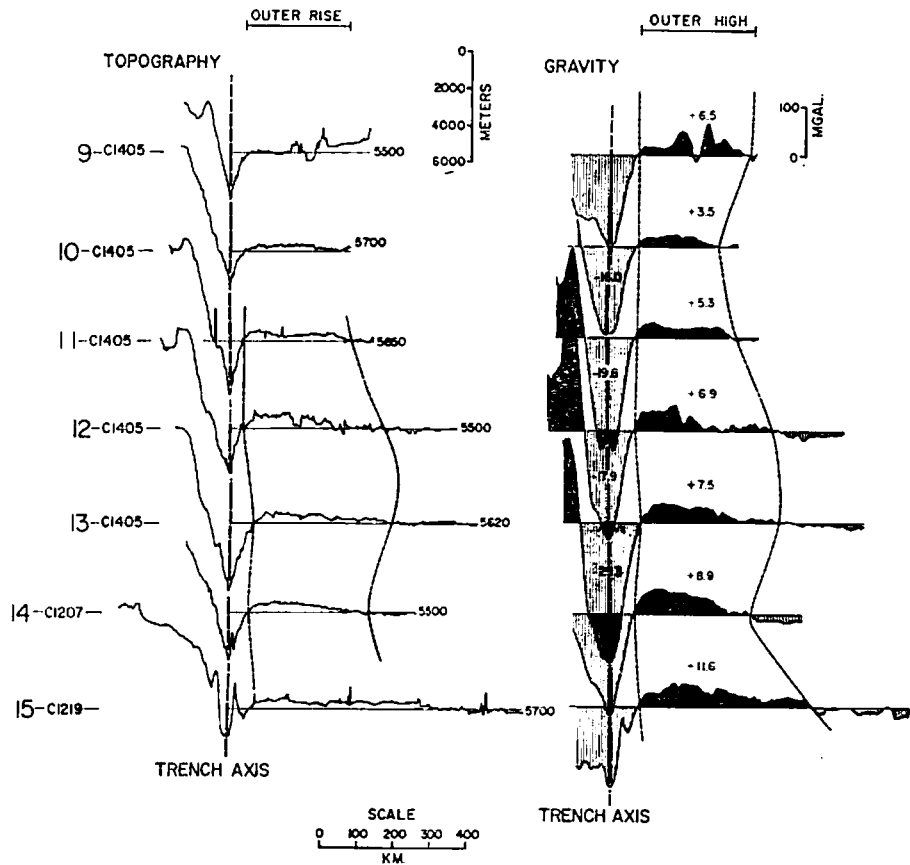


FIG. 3. Topography and gravity anomaly profiles 9-15 (Fig. 1) of the Kuril Trench. Note the close correlation of positive gravity anomalies with a regional rise in topography seaward of the trench.

described on profile 3. The regional rise in topography seaward of the trench also correlates with seismic reflection evidence of a regional rise in the acoustic basement (Hayes & Ewing 1970, Fig. 6). The irregularity of the sea floor makes it more difficult, however, to identify the amplitude and extent of the regional rise. We estimate a regional rise in the range 500-900 m for profiles 4, 5 and 6 (Fig. 2). There is good evidence that the regional rise narrows from east to west reaching a minimum width of about 350 km on profile 6.

Profiles 7 and 8 cross the western Aleutian Trench south of Attu Island. Profile 8 extends across the Aleutian Arc to the Bowers Basin which reaches mean depths of about 4 km. The trench is well developed on profiles 7 and 8 and is characterized by a relatively steep seaward wall of about 4° . The sea floor is irregular seaward of the trench although a regional rise in topography can be seen on profile 7. Profile 8, however, extends across the northern limits of the Emperor Seamount Chain which complicates identification of regional trends in topography seaward of the trench.

Gravity anomalies show a close correlation with the main features described on the topography profiles. The Aleutian Arc and the narrow shelf bordering the islands are associated with large amplitude positive anomalies of up to +184 mgal (Profiles 4 and 8, Fig. 2; Woollard & Rose 1963; Carr *et al.* 1971; Kienle 1971). The Aleutian

JAPAN - BONIN - MARIANA TRENCHES

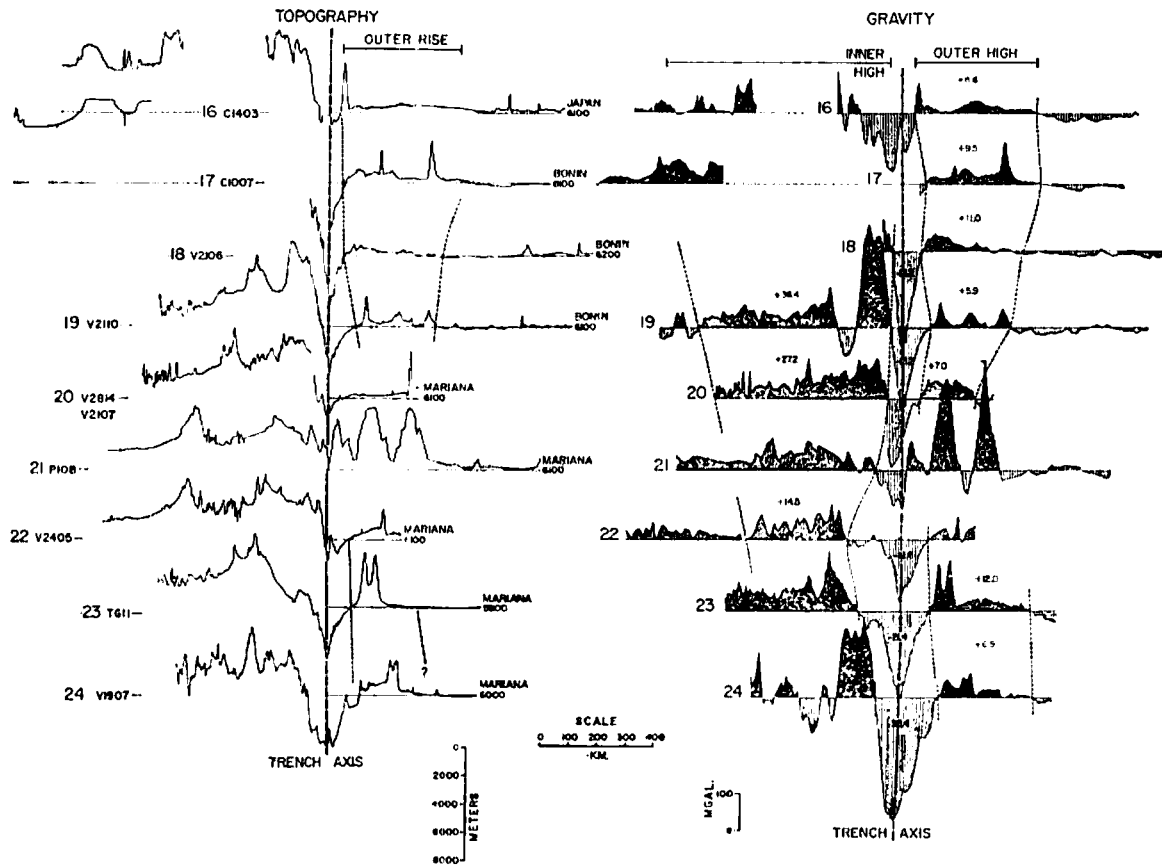


FIG. 4. Topography and gravity anomaly profiles 16-24 (Fig. 1) of the Japan, Bonin and Mariana Trenches. Note the relatively steep seaward wall of the trench and the outer rise in topography for profiles 16-18. In comparison, the seaward wall is shallower and the outer rise in topography reduced in amplitude for profiles 19-24. The significance of these observations is discussed in the text.

PHILIPPINE - RYUKYU - NANKAI TRENCHES

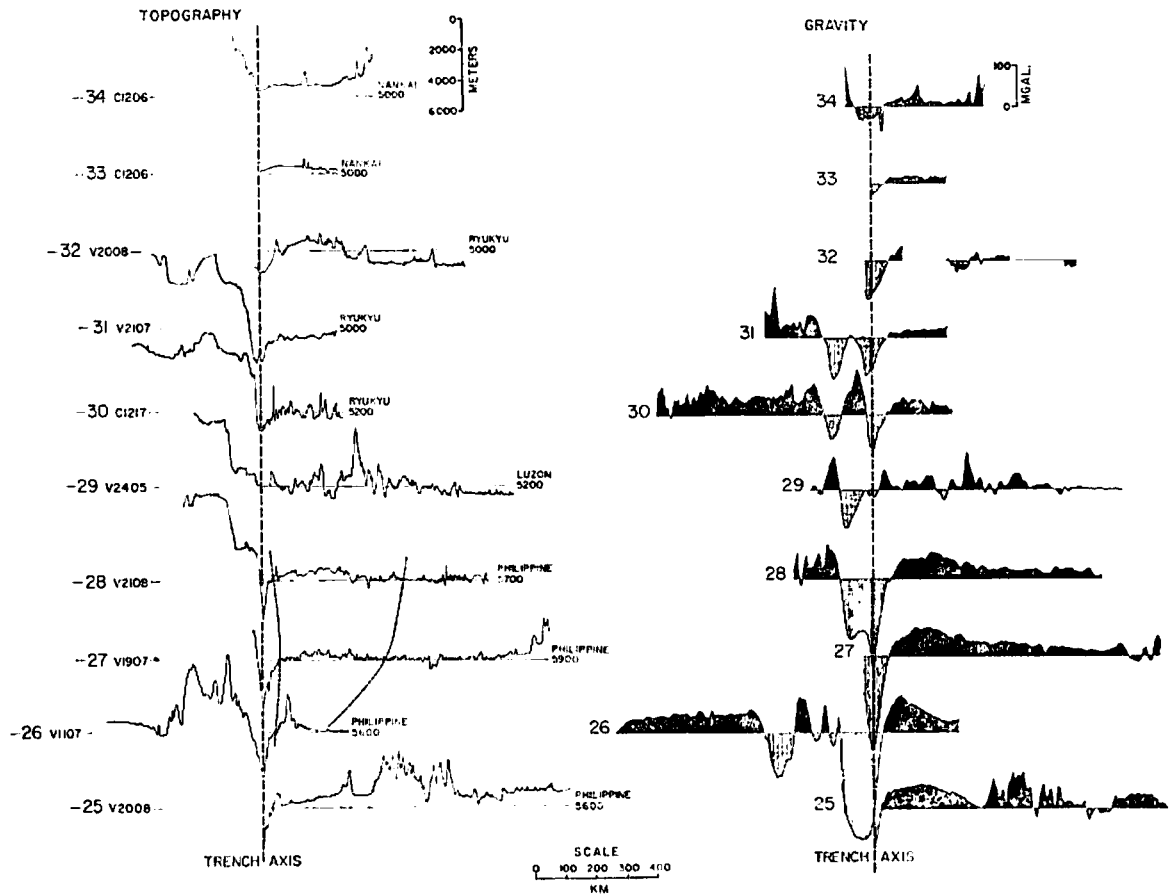


FIG. 5. Topography and gravity anomaly profiles 25-34 (Fig. 1) of the Philippine and Ryukyu Trenches and the Nankai Trough. The positive anomalies are well developed seaward of the Philippine Trench where they correlate with a regional rise in the topography.

Basin and Bowers Basin, landward of the arc (Profiles 4 and 8, Fig. 2; Kienle 1971), correlate with nearly zero anomalies. The Aleutian Trench correlates with large amplitude negative anomalies of about -187 mgal (Profiles 1 to 8, Fig. 2; Malahoff & Erickson 1969; Kienle 1971). We note that the negative anomalies are generally displaced landward of the landward wall of the trench (Hayes & Ewing 1970; Talwani 1970).

A striking feature of the gravity anomaly profiles, however, is the well-developed Outer Gravity High (Fig. 2). The Outer Gravity High is bordered to the north by the negative anomalies of the Aleutian Trench and to the south by near zero anomalies of the Pacific Ocean Basin. The Outer Gravity High reaches peak amplitudes of $+50$ to $+60$ mgal between 90 and 150 km seaward of the trench axis and decreases gently southwards. The width of the Outer Gravity High decreases westwards from about 600 km for profiles 2 and 3 (Fig. 2) to about 350 km for profile 7 (Fig. 2). There is generally a good correlation between the extent of the Outer Gravity High and the observed regional rise in topography seaward of the trench (Fig. 2).

Kuril Trench

Topography and free-air anomaly profiles of the Kuril Trench between 42° N and 52° N are presented in Fig. 3. The profiles represent data obtained during cruises of *Robert D. Conrad* seaward of the Kuril Islands.

Profile 9 crosses the northern part of the Kuril Trench east of Kamchatka Peninsula. The trench reaches depths of 7.9 km on this profile and is characterized by an irregular landward wall and a relatively steep seaward wall (about 3°). Seaward of the trench the profile crosses the northern extension of the Emperor Seamount Chain.

Profiles 10–14 cross the narrow shelf bordering the Kuril Islands, the Kuril Trench and the sea floor seaward of the trench. The landward wall of the trench is relatively smooth and characterized by slopes of up to 6° . The seaward wall of the trench is noticeably steep (about 3° to 5°). A maximum depth of the trench of 9.6 km is observed on profile 13. Seaward of the trench is a well developed regional rise in topography of a few hundred metres. The regional rise has also been outlined in Chase, Menard & Mammerickx (1970) where it is termed the Hokkaido Rise. The regional rise reaches an amplitude of 300–700 m above an estimated 'undisturbed' depth of the sea floor of 5.5 to 5.7 km between the Kuril Trench and the Emperor Seamount Chain.

Profile 15 crosses the relatively gentle wall of the Japan Trench between Hokkaido and Honshu and the Erimo Seamount near the boundary of the Kuril and Japan Trenches. A broad regional rise in the topography can still be distinguished seaward of the trench.

Gravity anomalies reach a peak amplitude of $+247$ mgal on the shelf adjacent to the Kuril Islands. Interpolation between two free air anomaly profiles across the Sea of Okhotsk (Gainanov 1955) suggest the anomalies observed on the shelf (Profiles 11, 12 and 13) may be the maximum values for the Kuril Arc. The positive anomalies decrease sharply towards the Kuril Trench to minimum values of -285 mgal on profile 13. We note that on profile 9 and other unpublished profiles that lie further north-east of the Kamchatka Peninsula, the negative anomalies are generally displaced landward of the landward wall of the trench.

An important feature of the gravity anomaly profiles, however, is the well-developed Outer Gravity High (Fig. 3). The Outer Gravity High reaches widths of 300–400 km (Fig. 1) and correlates with the regional rise in topography seaward of the trench (Fig. 3). For profile 13 (Fig. 3) an estimated regional rise in topography of 700 m is associated with a maximum gravity anomaly of about $+40$ mgal.

Japan–Bonin–Mariana Trenches

Topography and free-air anomaly profiles across the Japan, Bonin and Mariana Trenches are presented in Fig. 4. The profiles also include parts of the Japan Sea and eastern Philippine Sea.

Profiles 16–18 extend from the southern part of the Japan Trench to the southern Bonin Trench. The configuration of the trench on profile 16 is complicated by a small group of seamounts. Profiles 17 and 18 show depths of the trench of about 9.4 km and steep landward and seaward walls. Profiles 16 and 17 cross the NE–SW trending ridges associated with the eastern part of the Japan Sea. The Japan Sea reaches a mean depth of about 4 km between the ridges crossed on profiles 16 and 17. Seaward of the trench, profiles 16 and 17 show a regional rise in topography of 300–800 m. The regional rise is also well seen on profile 18 (Fig. 4) where it compares closely to the regional rise in topography of profiles seaward of the Kuril and Aleutian Trenches (Figs 2 and 3).

Profiles 19–24 cross the system of linear ridges and narrow basins described in Vening Meinesz (1964), Menard (1964) and Karig (1971b) landward of the Bonin and Mariana Arcs. The distance between the island arc and the first linear ridge landward of the arc increases from about 60 km on profile 19 to about 250 km on profile 22 (Fig. 4). The narrow basins are characterized by an irregular sea floor (Fig. 4) and thin sediments and probably formed by processes of crustal extension (Karig 1971b).

Profiles 19–24 cross the southern part of the Bonin and Mariana Trenches. The depth of the trench on profile 19 reaches 9.4 km. We note that the slope of the seaward wall of the trench is relatively gentle on profiles 19–24 compared to profiles 17 or 18 (Fig. 4).

Profiles 19–24 are, however, complicated by the westerly extent of the Mid-Pacific Seamount Chain (Menard 1964). Where the regional topography can be distinguished (for example Profiles 20 and 23, Fig. 4) the regional rise seaward of the trenches is reduced in width and amplitude compared to profiles 17 and 18 and to profiles seaward of the central and eastern Aleutian and Kuril Trenches.

Gravity anomaly profiles show that maximum positive anomalies occur in the vicinity of the Bonin and Mariana Arcs and decrease gradually landward of the arcs. We note that the eastern part of the Japan Sea (Tomoda *et al.* 1970) and the Philippine Sea (Profiles 19–23) are associated with generally positive anomalies. These positive anomalies are regional in extent and do not appear to be localized over the narrow inter-arc basin as suggested by Karig (1971a) westward of the Bonin and Mariana Arc.

Gravity anomalies reach minimum values of -322 mgal across the Mariana Trench (Profile 24, Fig. 4). We note that for profiles 22–24 the minimum of the negative anomalies correlates with the axis of the deep-sea trench.

Gravity anomaly profiles show the Outer Gravity High is well developed seaward of the northern Bonin Trench (Profiles 17 and 18, Fig. 4) where it is similar in both amplitude and wavelength to the Outer Gravity High seaward of the central Aleutian and Kuril Trenches. The Outer Gravity High cannot, however, be clearly seen on Profiles 19, 21 and 22 seaward of the southern Bonin and Mariana Trenches. These profiles are complicated by the gravity effect of local irregularities in topography associated with the western extent of the Mid-Pacific seamount chain (Fig. 4). We can, however, distinguish the Outer Gravity High on profiles 20, 23 and 24 (Fig. 4) seaward of the southern Bonin and Mariana Trenches. The Outer Gravity High seaward of these trenches is relatively narrow compared to the northern Bonin (Profiles 17 and 18, Fig. 4) and the central Aleutian and Kuril Trenches (Figs 2 and 3).

Philippine-Ryukyu-Nankai Trenches

Topography and free-air gravity profiles of trenches in the western Philippine Sea are presented in Fig. 5. The profiles also extend to part of the Okinawa Trough and the Celebes Sea.

Profiles 25-28 (Fig. 5) cross the well-developed Philippine Trench east of the Philippine Islands. The trench reaches depths comparable to the Mariana Trench and is associated with steep (6° to 8°) seaward walls (Fig. 5; Fisher & Hess 1965). Seaward of the trench the sea floor is irregular and is characterized by a broad regional rise in topography (Profiles 27 and 28, Fig. 5). The trench terminates abruptly at about 15° N where it passes into the steep continental slope east of Luzon (Profile 29, Fig. 5).

Profiles 30, 31 and 32 cross the Ryukyu Trench and the Okinawa Trough landward of the Ryukyu Islands. We note that the trench is not as well developed as for the Philippine Trench. However, the landward walls of both trenches are steep. There is no evidence on profiles 30 and 31 of a regional rise in topography seaward of the trench.

Profiles 33 and 34 cross the Nankai Trough south of the Kii Peninsula in south-west Japan. The trench is poorly developed on these profiles and reaches depths of about 4-7 km. Seismic reflection profiles and sediment studies (Hilde, Wageman & Hammond 1969) indicate the Nankai Trough is probably a geologically recent feature, less than 1 My in age.

The Philippine Trench is associated with large amplitude negative gravity anomalies (Profiles 26, 27 and 28, Fig. 5). We note that the minimum negative anomalies are displaced landward of the trench axis. The Ryukyu Trench is associated with a negative anomaly which is bordered by a small positive anomaly and another large negative anomaly over a bench in the landward wall (Profiles 30 and 31). The amplitudes of the negative anomalies are substantially smaller than for the Philippine Trench. Smaller amplitude negative anomalies of about -60 mgal correlate with the Nankai Trough (Profiles 33 and 34, Fig. 5).

An important feature of the gravity anomaly profiles, however, is the well-developed Outer Gravity High seaward of the Philippine Trench. The Outer Gravity High correlates with the broad regional rise in topography seaward of the trench (Fig. 5) and is similar in amplitude to the Outer Gravity High seaward of the Aleutian and Kuril Trenches. The Outer Gravity High cannot be easily distinguished seaward of the Ryukyu Trench or the Nankai Trough (Fig. 5).

Interpretation of the Outer Gravity High

The Outer Gravity High is well developed seaward of deep-sea trenches in the north-western Pacific. We have noted there is a close correlation between the Outer Gravity High and a regional rise in topography seaward of trenches (Figs 2-5). In this section we examine the correlation in more detail.

Correlation between free-air gravity anomalies and topography

The correlation between free-air anomalies and topography for three theoretical crustal models seaward of trenches is shown in Fig. 6.

Model 1 assumes the regional rise in topography is in isostatic equilibrium according to the Airy-Heiskanen hypothesis. There would be little or no correlation with gravity anomalies for this model.

Model 2 assumes the regional rise is uncompensated at depth. The change in gravity anomaly for this model is about 7.0 mgal for each 100 m change in elevation.

Model 3 assumes there is no change in crustal thickness beneath the trench and regional rise. The change in gravity anomaly of this model is caused by warping of

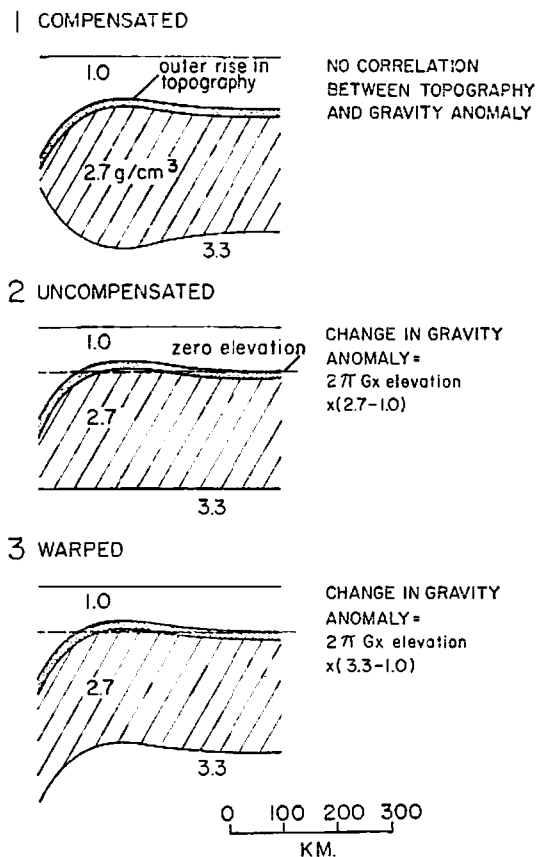


FIG. 6. Correlation of gravity anomalies and topography expected for three theoretical crustal models of the regional rise in topography seaward of trenches. The change in gravity anomaly for Models 2 and 3 is shown assuming the thickness of the sediment layer (indicated by stippling) is unchanged seaward of the trench.

individual crustal layers and the crust-mantle boundary and is about 9.5 mgal for each 100 m change in elevation.

The correlation of the observed Outer Gravity High with topography is, however, sufficiently close (Figs 2, 3 and 4) to make Model 1 an unlikely explanation of crustal structure beneath the regional rise. Before considering Models 2 and 3, however, we need to consider other possible sources which could contribute to the Outer Gravity High. A possibility is a gravity 'edge effect' of a dense downgoing slab.

Gravity effect of a dense downgoing slab

Seismic evidence indicates an inclined zone of material characterized by low attenuation of body waves beneath island arcs (Oliver & Isacks 1967; Jacob 1972). Focal mechanism solutions of shallow earthquakes (Stauder 1968) suggest the zone is produced by the downward movement of lithospheric plates relative to island arcs.

The low attenuation of body waves indicates the zone is relatively cold and dense and should give rise to long wavelength positive gravity anomalies (Oxburgh & Turcotte 1970; Griggs 1972). The positive anomalies could contribute to the regional gravity field landward of island arcs (Hatherton 1969, 1970) and the Outer Gravity High seaward of trenches.

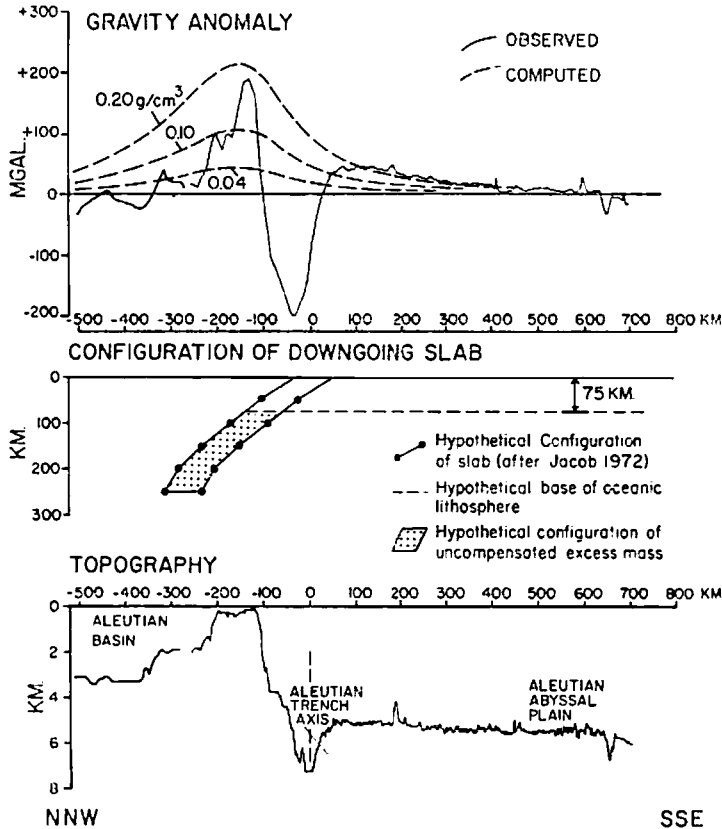


FIG. 7. Computed gravity effect of a dense downgoing slab beneath the Aleutian Arc compared to profile 4 (Fig. 1). Computations are shown assuming uniform density contrasts of $+0.04$, $+0.10$ and $+0.20 \text{ g cm}^{-3}$ for the slab. Note that to fully explain the positive anomalies seaward of the trench a uniform density contrast of at least $+0.20 \text{ g cm}^{-3}$ is required for the slab.

Computation of the gravity effect of the dense downgoing slab beneath island arcs is complicated by the unknown density distribution and configuration of the slab. There is also a problem of whether the slab is regionally compensated (Griggs 1972). Thermal studies (Minear & Toksöz 1970; Oxburgh & Turcotte 1907) show a complex distribution of temperature within the downgoing slab which depends strongly on the underthrusting rates assumed. These temperature distributions give rise to complex lateral and vertical density contrasts within the slab.

In this study we consider the gravity effect of a downgoing slab beneath the Aleutian Arc. The Aleutian Arc was chosen because (1) the slab configuration is relatively well known from the seismic studies of Jacob (1972), and (2) the Outer Gravity High is well developed seaward of the Aleutian Trench and relatively undisturbed by local irregularities in topography (Fig. 2).

In the computations it is necessary to assume the configuration and physical properties of the downgoing slab. In this study we use the slab configuration obtained by Jacob (1972) from P -wave travel-time residuals of the nuclear explosion Longshot. We use his model LS 107 with a plate thickness of 80 km. This model places the downgoing slab nearest to the trench and will give a maximum likely estimate of the gravity effect in the region of the Outer Gravity High. The density contrast between the slab and surrounding asthenosphere is assumed uniform and to extend the full

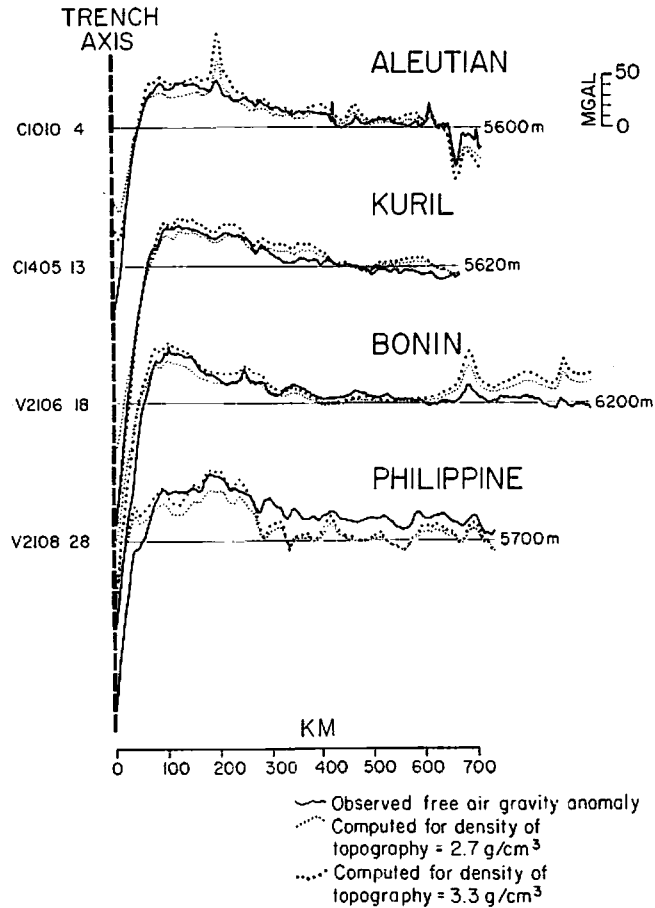


FIG. 8. Gravity effect of the topography seaward of trenches for assumed crustal densities of 2.7 g cm^{-3} and 3.3 g cm^{-3} compared to observed profiles. Note the excellent correlation between the computed gravity effect and the observed positive anomalies seaward of the trench.

length of the slab beneath 75 km. This is the approximate thickness of the oceanic lithosphere (Kanamori & Press 1970). In addition, we assume the slab can be approximated to a two-dimensional body on a spherical Earth.

The comparison of the computed gravity effects with observed profile 4 (Fig. 2) are shown for assumed uniform density contrasts for the slab of $+0.04$, $+0.10$ and $+0.20 \text{ g cm}^{-3}$ (Fig. 7). The computations show that to match the amplitude of the Outer Gravity High a uniform density contrast of *at least* $+0.20 \text{ g cm}^{-3}$ is required. A higher uniform density contrast would be required if the slab is regionally compensated or if it is located farther landward from the trench.

There are, however, difficulties with a model that assumes a uniform density contrast of at least $+0.20 \text{ g cm}^{-3}$ for the downgoing slab. The computed model predicts positive anomalies of the order of $+100 \text{ mgal}$ across the Aleutian Basin compared to observed values which are near zero (Profiles 4 and 8, Fig. 2; Kienle 1971). In addition, the uniform density contrast of $+0.20 \text{ g cm}^{-3}$ required for the slab is substantially higher than mean uniform density contrasts suggested by Oxburgh & Turcotte (1970) and used in computations by Griggs (1972). Oxburgh & Turcotte (1970) suggest that the complex density distribution in the slab is equivalent to a

uniform density contrast of about $+0.04 \text{ g cm}^{-3}$ for an underthrusting rate of 8 cm/yr or $+0.01 \text{ g cm}^{-3}$ for 1 cm/yr . Since the underthrusting rate for the Aleutian Arc is about 6 cm/yr (LePichon 1968) the density contrast for the downgoing slab may not exceed $+0.04 \text{ g cm}^{-3}$.

We note that for an assumed density contrast of $+0.04 \text{ g cm}^{-3}$ for the downgoing slab the maximum gravity effect in the vicinity of the Outer Gravity High would be only 5 mgal (Fig. 7). These observations suggest that a dense downgoing slab beneath the Aleutian Arc is unlikely to contribute significantly to the Outer Gravity High. With this result we can now examine the correlation of the Outer Gravity High with topography in more detail.

Gravity effect of topography

Gravity anomaly profiles have been examined seaward of trenches where the regional rise in topography is well developed. The principal term in the gravity effect of the topography can be obtained from

$$2\pi \cdot G \cdot \Delta\rho \cdot (\bar{H} - H) \quad (1)$$

where $\Delta\rho$ = density difference between sea water and crustal rocks, \bar{H} = estimated depth of undisturbed sea floor seaward of the outer rise and H = depth of the sea floor. The estimated values of \bar{H} are shown for the profiles selected in Fig. 8.

The gravity effect of topography for assumed crustal densities of 2.7 and 3.3 g cm^{-3} are shown in Fig. 8. There is an excellent correlation between the computed effect for these crustal densities and the observed Outer Gravity High (Fig. 8). We note there are local differences in the fit near irregularities in topography but the gravity effect of the topography generally explains both the wavelength and amplitude of the Outer Gravity High. There is a small disagreement seaward of the Philippine Trench which may be due to a local positive regional background field.

The assumed crustal densities of 2.7 and 3.3 g cm^{-3} correspond to Models 2 and 3 shown in Fig. 6. Due to uncertainties in the depth of the 'undisturbed' sea floor seaward of the regional rise it is not possible on the basis of gravity observations alone to distinguish between Models 2 and 3. In the next section we discuss evidence that the crustal upwarp model (Model 3, Fig. 6) is the most likely explanation of the Outer Gravity High seaward of trenches.

The Outer Gravity High and simple models of flexure of the oceanic lithosphere at island arcs

It is generally accepted that some form of thermal convection is the driving force of plate motions. However, it is not clear whether lithospheric plates play an active role above a weak asthenosphere (Lliboutry 1969; Jacoby 1970; Elsasser 1971) or a passive role above convection cells in the asthenosphere (Schubert & Turcotte 1972).

The forces which prevail on an oceanic plate approaching a deep-sea trench are important in studies of gravity anomalies seaward of trenches. If the approaching plate is coupled to the downgoing slab beneath island arcs and there is no resistance to the downward motion the 'pull' of a dense sinking slab would be expected to transmit a tensile force to the approaching plate. This tensile force may, however, be negated if the sinking slab is de-coupled from the approaching plate by fracturing (Lliboutry 1969; Kanamori 1971; Abe 1972) or if an equal or greater compressive force is applied to the plate. Such a force could be provided as a 'push' from an uplifted mid-ocean ridge (Jacoby 1970) or by a motion of the plate landward of the trench which opposes the motion of the approaching plate (Elsasser 1971). If the tensile forces are negated, compressive forces may be transmitted to the oceanic plate.

Simple models for the forces acting on an oceanic plate approaching a deep-sea trench have been considered by Lliboutry (1969) and Hanks (1971). Lliboutry (1969) discussed the position of the trench in relation to the island arc by applying an oblique force to the edge of an approaching oceanic plate. Hanks (1971) however, discussed the regional rise in topography observed seaward of the Kuril trench by applying vertical and horizontal components of force on the edge of the plate. Both studies assumed the oceanic lithospheric plate could be modelled as a semi-infinite elastic sheet overlying a weak fluid asthenosphere. The viscosity of the asthenosphere can be neglected in the computations since the age of the deformation is significantly greater than the response time of the asthenosphere indicated from studies in the vicinity of ice loads. Such models using both semi-infinite and continuous elastic sheets have also been used in studies of the deformation of the lithosphere associated with sea-mounts and sediments (Gunn 1943; Walcott 1970).

In this study we consider a similar model for an oceanic plate approaching an island arc as considered by Hanks (1971). We use this model to obtain the deflection of an oceanic plate approaching island arcs in the north-western Pacific. In addition, since the gravity effect of the deflection can be computed, comparisons are made to the gravity anomalies associated with the trench and with the Outer Gravity High seaward of trenches.

Theory of method

The general equation for the deflection of an elastic sheet is a well-known problem in engineering and is given by (Hetényi 1946)

$$EI \cdot \frac{d^2 y}{dx^2} = M \quad (2)$$

where E is the modulus of elasticity of the sheet, I is the cross-sectional moment of inertia of the sheet at a point on the x axis and M is the bending moment at a point x about a fixed point. The product EI is a measure of the stiffness of the sheet and is defined as D , the effective flexural rigidity. The co-ordinate system is chosen so that the x axis is parallel to the undisturbed axis of the sheet and that deflections occur in the $x-y$ plane.

In the application of elastic sheets to the Earth the bending moment, M is usually unknown. However, its second derivative, the restoring stress, can be expressed in terms of buoyancy forces. In the absence of applied forces we have

$$\frac{d^2 M}{dx^2} = (\rho_m - \rho_w) \cdot y \cdot g \quad (3)$$

where ρ_m is the density of material underlying the sheet, ρ_w is the density of material infilling the deflection and g is average gravity.

The equation for the deflection of a continuous elastic sheet is then obtained from (2) and (3) as

$$EI \cdot \frac{d^4 y}{dx^4} - (\rho_m - \rho_w) \cdot y \cdot g = 0. \quad (4)$$

The solution of (4) gives four constants of integration which can be determined from the boundary conditions of the problem. For the boundary conditions that the deflection is zero for great distances and the sheet is semi-infinite with a free edge at the origin we get (Hetényi 1946, p. 24)

$$y = \frac{2P_b \lambda \cdot \exp(-\lambda x) \cdot \cos \lambda x}{(\rho_m - \rho_w) \cdot g} \quad (5)$$

where P_b is a vertical force/unit width applied at the origin.

The deflection curve is a damped sinusoidal curve with a wavelength equal to $2\pi/\lambda$. The damping factor λ has been termed the 'lithospheric constant' by Gunn (1943) and $1/\lambda$ the 'flexural parameter' by Walcott (1970). λ is given by

$$\lambda = \sqrt[4]{\left(\frac{(\rho_m - \rho_w) \cdot g}{4D}\right)}. \quad (6)$$

A problem in the application of the deformation models to island arc and deep-sea trenches is that the applied force P_b cannot be expressed in terms of a known surface load. We can, however, estimate P_b if the deflection is assumed at one point along the sheet (Hanks 1971). A known point on the deflection curve is the maximum depth of the trench beneath the depth of the 'undisturbed' sea floor which we denote Y_0 . If this occurs at $x = 0$ we then have from (5)

$$P_b = \frac{Y_0 \cdot (\rho_m - \rho_w) \cdot g}{2\lambda}. \quad (7)$$

With

$$D = 1.7 \times 10^{30} \text{ dyne cm}$$

$$\rho_w = 1.03 \text{ g cm}^{-3}$$

$$\rho_m = 3.3 \text{ g cm}^{-3}$$

$$g = 980 \text{ cm s}^{-2}$$

$$Y_0 = 4 \text{ km}$$

in (6) and (7) we get

$$\lambda = 74.6 \text{ km}$$

and

$$P_b = 0.33 \times 10^{16} \text{ dyne cm}^{-1}. \quad (8)$$

We have assumed a similar value for D as considered by Hanks (1971). It is unlikely that this value varies by more than a factor of 5 for ages of loading greater than a few million years (Walcott 1970).

The deflection curve for the parameters in (8) is shown in Model A (Fig. 9). The deflection is positive for distances between 176 and 310 km. This region is termed the peripheral bulge and is an important feature of the flexure models. The amplitude of the bulge depends only on the magnitude of the applied force P_b .

We can also estimate the magnitude of the bending stresses in the sheet once the deflection curve is known. The bending stress is given by

$$(S)_{\max} = \frac{ET}{2} \cdot \frac{d^2 y}{dx^2} \quad (9)$$

where E is Young's Modulus and T is the effective thickness of the sheet. T is related to the elastic parameters assumed for the sheet and for a Poisson's ratio σ is given by

$$T = \sqrt[3]{\left(\frac{12 \cdot D(1 - \sigma^2)}{E}\right)}. \quad (10)$$

With

$$D = 1.7 \times 10^{30} \text{ dyne cm}$$

$$E = 10^{12} \text{ dyne cm}^{-2}$$

$$\sigma = 0.25$$

we get

$$T = 27 \text{ km}. \quad (11)$$

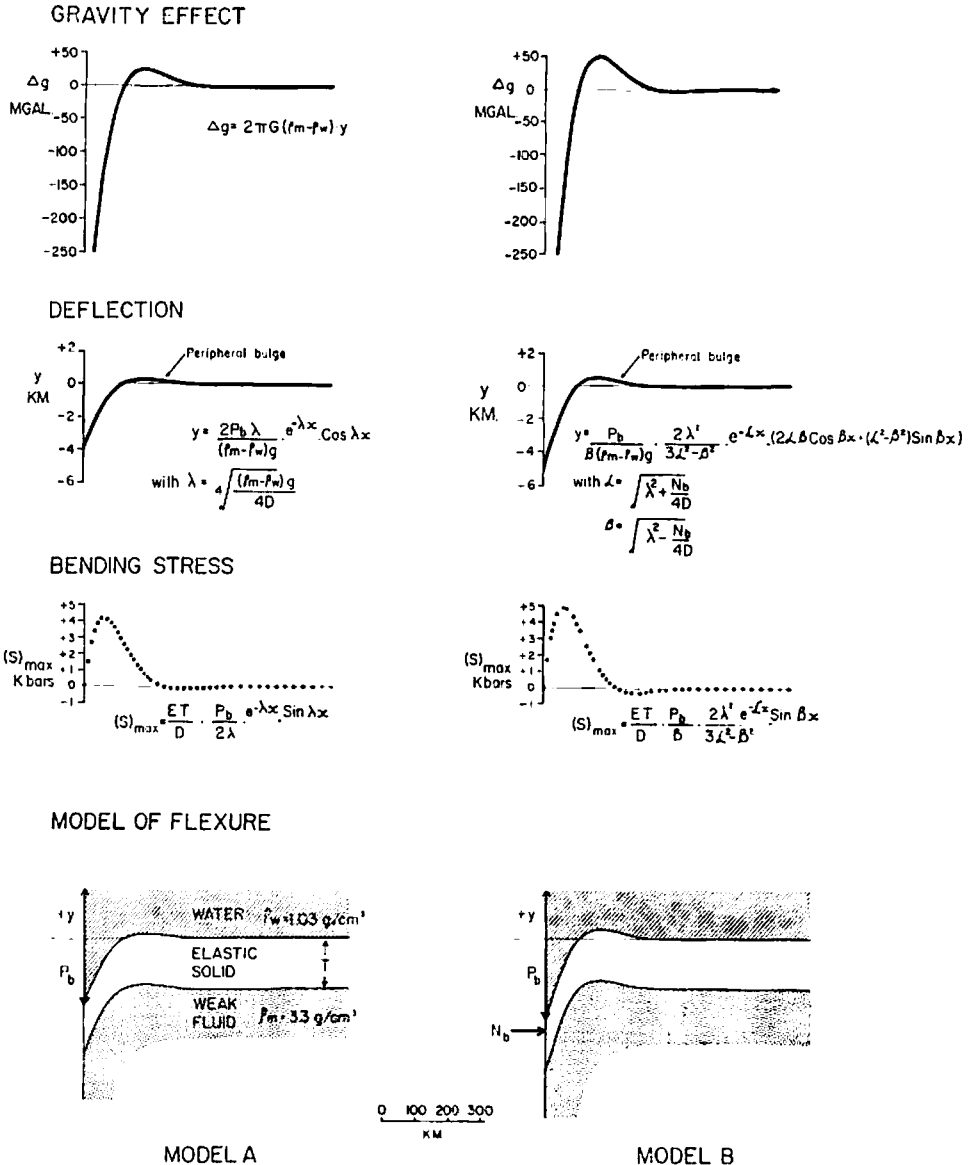


FIG. 9. Gravity effect, deflection curves and bending stresses for two simple models of flexure of an oceanic lithospheric plate approaching an island arc. The oceanic plate and underlying asthenosphere are modelled as an elastic solid overlying a weak fluid. Model A corresponds to the case of an applied vertical concentrated force only and Model B the case of a vertical and horizontal compressive force. We assumed values of $P_b = 0.33 \times 10^{16}$ dynes cm^{-1} and $N_b = 0.17 \times 10^{17}$ dynes cm^{-1} for the models. The equations for the deflection curves are based on Hetényi (1946). Note the occurrence of a peripheral bulge, beyond the main deflection in Models A and B, which correlates with positive gravity anomalies.

We note the thickness of the sheet assumed to compute the bending stresses is an effective thickness and may not correspond to the actual thickness of the lithosphere.

The bending stress has been determined for Model A (Fig. 9) for an assumed effective thickness of the plate of 27 km. A maximum bending stress of about 4 kbar occurs 55 km from the computational origin. The curvature of the plate at this

point indicates that the upper part of the plate is in tension while the lower part is in compression.

In discussion of the deflection curves and stresses within the plate we have only considered an applied vertical force at the origin (Model A, Fig. 9). It is also possible to determine the deflection curves and stresses in the plate for the case of an additional axial compressive or tensile force applied at the origin. This case was also considered by Hanks (1971) and is shown in Model B (Fig. 9). The deflection curves and bending stresses in the plate have been obtained from equations given in Hetényi (1946, p. 130) using the parameters listed in (8) and (11). In Model B a horizontal compressive force has been assumed which is about 5 times the vertical force P_v .

ALEUTIAN-KURIL-BONIN-MARIANA TRENCHES

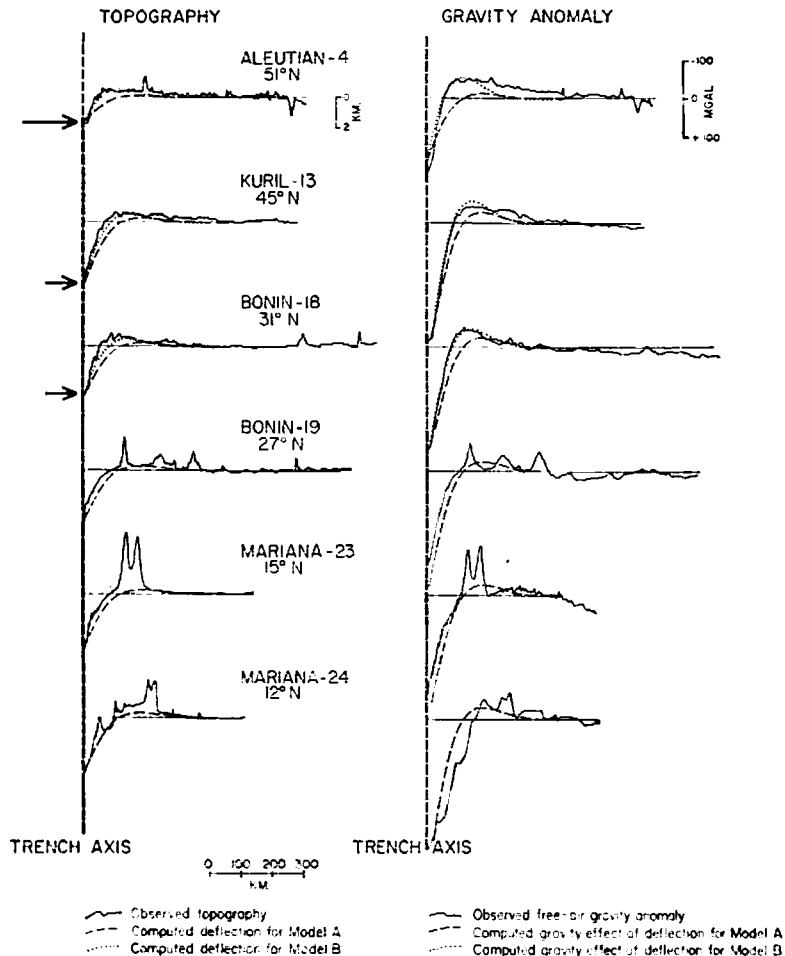


FIG. 10. Comparison of gravity effect and deflection curves for Models A and B (Fig. 9) to observed gravity anomaly and topography profiles seaward of trenches in the north-west Pacific. Profiles across the Mariana and southern part of the Bonin Trenches can be adequately explained by Model A (Fig. 9). Profiles across the northern part of the Bonin Trench and the Kuril and central and eastern Aleutian Trenches, however, can be best explained by Model B (Fig. 9). The length of the arrow is proportional to the magnitude of the compressive stresses acting on the oceanic plate.

The differences between the deflection curves of Models A and B (Fig. 9) are important in the application to island arcs. The introduction of a horizontal compressive force shifts the deflection curves down and therefore to retain the point $(0, y_0)$ on the deflection curve, the entire curve has to be shifted to the left (Hanks 1971). For Model B (Fig. 9) the shift is about 15 km. In addition, the deflection curve for Model B is noticeably steeper and the estimates of the bending stress larger. We also note that the amplitude of the peripheral bulge is larger for Model B than for Model A.

Gravity effect of simple models of flexure

The application of surface loads on an elastic plate produces deflections which are associated with gravity anomalies. The total gravity anomaly associated with a flexural model is obtained from the combined gravity effect of the surface load and the deflection. Since the deflection curve is a form of compensation for the applied surface load the total gravity effect of the model integrated to great distances will be zero.

The flexure Models A and B (Fig. 9), however, are associated with boundary forces and not a surface load. The total gravity effect of the models is then obtained from the gravity effect of the deflection curves. The principal term in the gravity effect is given by

$$\Delta g = 2\pi G \cdot (\rho_m - \rho_w) \cdot y \quad (12)$$

where y is the deflection and ρ_m and ρ_w have been previously defined.

A large amplitude negative gravity anomaly of about -380 mgal correlates with the point of application of the applied force. Positive anomalies of up to $+26$ and $+52$ mgal correlate with the peripheral bulge.

The total gravity effect of Models A and B (Fig. 9) is significantly negative. For Model A the integrated profile is -14×10^3 mgal km. It is not zero as in the case of a deformation due to surface load where the surface load itself contributes to the total gravity effect. As we would expect the total gravity effect -14×10^3 mgal km exactly balances a surface load equivalent to the vertical force P_b . The mass of a load equivalent to P_b is simply P_b/g and the gravity effect is given by

$$\Delta g_t = \frac{2\pi G P_b}{10^3 \cdot g} \quad (13)$$

with

$$G = 6.67 \times 10^{-8} \text{ c.g.s.}$$

$$g = 980 \text{ cm s}^{-2}$$

$$P_b = 0.33 \times 10^{16} \text{ dynes cm}^{-1}$$

This gives a value for the gravity effect of the equivalent load of $+14 \times 10^3$ mgal km.

Comparison of simple models to the Outer Gravity High

The comparison of simple models of flexure to observations is complicated by two main problems. First, the origin of the applied forces is unknown and second, more than one system of applied forces may explain the observations. These problems have been discussed by Walcott (1970a) and Hanks (1971).

In this study we utilize the assumptions of Hanks (1971) that the origin of the computations is located at the trench axis and that the applied forces causing the deflection of the plate can be resolved into a simple system of vertical and horizontal components of force. We can then determine whether the Outer Gravity High

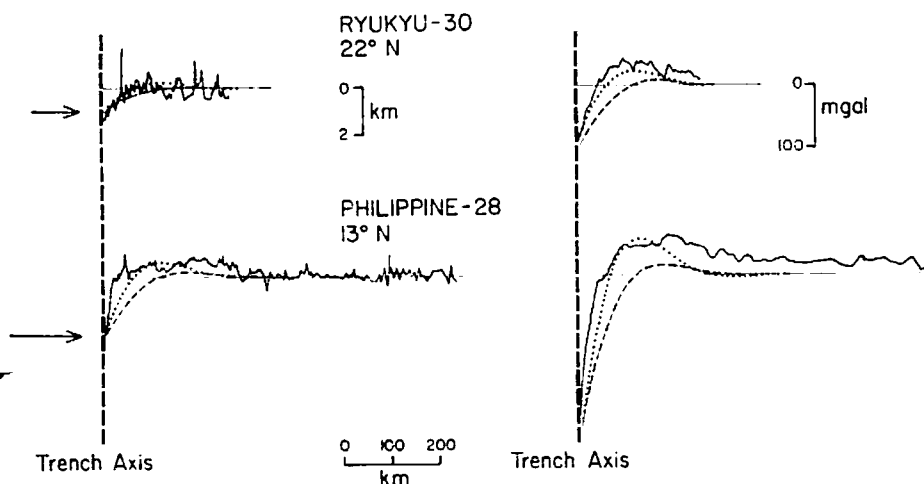


FIG. 11. Comparison of gravity effect and deflection curves for Models A and B (Fig. 9) to observations seaward of trenches in the western Philippine Sea. The computed effects are similar to the key shown in Fig. 10. Note that Model A cannot satisfactorily explain profiles across the Philippine or Ryukyu Trenches. Model B is an improved fit although there is a significant discrepancy between the extent of the observed Outer Gravity High and the computed profiles.

can be explained by simple models of flexure of an elastic oceanic plate which is approaching an island arc.

The comparison of simple models of flexure to observations seaward of trenches is shown in Figs 10 and 11. The simple models correspond to Models A and B (Fig. 9) and assume parameters listed in (8) and (11). The observed profiles have been selected from Figs 2 to 5. The selected profiles have been chosen to be (1) representative of each trench system, and (2) relatively free of short-wavelength irregularities in topography and gravity anomalies seaward of the trench.

The comparison shows that the computed deflection curves for Model A (Fig. 9) satisfactorily explains selected profiles 19, 23 and 24 seaward of the southern Bonin and Mariana Trenches (Fig. 10). The computed profiles explain the relatively shallow seaward wall of the trench and the poorly developed regional rise in topography and Outer Gravity High seaward of trenches (Fig. 10).

We note, however, that Model A does not satisfactorily explain the steep seaward walls or the large amplitude regional rise and Outer Gravity High of selected profiles 4, 13, 18, 28 and 30 of the central and eastern Aleutian, Kuril, northern Bonin, Ryukyu and Philippine Trenches. In order to explain these profiles it is necessary to either move the computational origin significantly landward of the trench axis or to consider a different system of forces at the origin. The profiles cannot be explained by varying the effective flexural rigidity of the plate in Model A. If the effective flexural rigidity is reduced, the wavelength of deflection decreases (and the seaward wall of the profile steepens) while the amplitude of the peripheral bulge is unchanged.

The profiles seaward of the central and eastern Aleutian, Kuril, northern Bonin and western Philippine Sea Trenches can be more satisfactorily explained by flexure models which include an additional horizontal compressive force at the origin. The computed profiles for Model B (Fig. 9) explains in a general way the observed steep seaward wall, large amplitude outer rise in topography and the Outer Gravity High seaward of these trenches. The fit between observed and computed profiles is generally good for profiles seaward of the Kuril and northern Bonin Trenches (Fig. 10). Hanks (1971) obtained a similar fit for a topography profile seaward of the Kuril Trench. The flexure model does not, however, fully explain the extent of the Outer Gravity

High seaward of the central and eastern Aleutian or the Philippine Trenches (Figs 10 and 11). The discrepancy for the central and eastern Aleutian Trench may be caused in part by a local ponding of uncompensated sediments south of Kodiak Island (Jones *et al.* 1971). Seismic reflection profiles in the vicinity of profile 4 (Jones *et al.* 1971) suggest the flexure of the acoustic basement (which is similar in amplitude but smaller in extent than the observed regional rise in topography) would explain the computed profiles more completely. However, another possibility is of an additional uplift of the oceanic plate seaward of the trench not predicted by the elastic flexure models. This may be due to the return flow of asthenospheric material responding to displacement by the downgoing slab. The discrepancy seaward of the Philippine Trench may be related to a positive regional background field associated with the Philippine Sea. This may also explain the relatively poor correlation between the gravity effect of the regional rise in topography seaward of the trench and the Outer Gravity High (Fig. 8).

We also note, however, that a horizontal compressive force applied at the origin is not uniquely required to explain observations seaward of the central and eastern Aleutian, Kuril, northern Bonin, Ryukyu and Philippine Trenches. A bending moment at the origin will also provide a component of horizontal compressive force acting on the oceanic plate and will reduce the magnitude of the horizontal compressive force required (Hanks 1971).

Stress estimates

The boundary stresses acting on the plate assumed for the computed profiles in Figs 10 and 11 have been summarized in Table 2. The stresses have been normalized to an effective plate thickness of 27 km. The vertical stresses required are of the order of 1 kilobar and the horizontal compressive stresses are of the order of 6 to 13 kbar (Table 2).

The maximum bending stresses in the plate have also been summarized in Table 2. The maximum bending stresses are of the order of 2–5 kbar and occur about 60 km seaward of the trench axis. The curvature indicates the upper part of the plate in the vicinity of the seaward wall of the trench is in tension and the lower part is in compression.

We would expect the materials of the plate to yield to the compressions and extensions. Extensional features have been described in the vicinity of trenches in the north-western Pacific. Stauder (1968) has reported a number of tensional focal mechanisms of shallow earthquakes in the vicinity of the seaward wall of the central and eastern Aleutian Trench. He attributes these mechanisms to a flexure of the

Table 2
Stresses acting on the oceanic plate and within the plate for computed profiles in Figs 10 and 11

Profile identification	Maximum depth of trench Y_0 metres	<i>Stresses acting on the plate</i>		<i>Stresses within the plate</i>
		Vertical stress P_b/T bars	Horizontal compressive stress N_b/T bars	Maximum bending stress (S) bars
Aleutian—4	1662	481	12950	2623
Kuril—12	3936	1220	6280	4938
Bonin—18	3235	1000	6650	4107
Bonin—19	3213	1000	—	3345
Mariana—23	3650	1100	—	3800
Mariana—24	2595	777	—	2696
Philippine—28	2563	777	7400	3781
Ryukyu—30	1000	259	11100	1300

downgoing Pacific plate. Shimazaki (1972) has reported a tensional focal mechanism about 60 km seaward of the Kuril Trench axis. Ludwig *et al.* (1966) has described evidence of normal faulting from seismic reflection profiles of the Japan Trench. The faults appear to disrupt both the sediments and the underlying acoustic basement.

However, it is most uncertain how the materials of the plate would respond to horizontal compressive stresses of the order of a few kilobars suggested in Hanks (1971) and this study. It is unlikely, for example, the materials of the upper part of the plate could sustain tensile stresses under compressive stresses of the order of a few kilobars since the principal horizontal stresses in both the upper and lower part of the plate would be compressive. Thus to explain the abundance of extensional features seaward of the central and eastern Aleutian Trench we may have grossly overestimated the horizontal compressive stress. It is also unlikely the materials of the plate would deform perfectly elastically in response to applied stresses of the order of a few kilobars. Rather, the plate would deform plastically. The effect of plastic flow produces a permanent deformation not predicted by the elastic models and would complicate the comparison of observed and computed profiles in Figs 10 and 11.

Clearly we have outlined a number of problems with the simple elastic flexure models. In particular, we may have grossly overestimated the magnitude of the applied horizontal compressive stresses (Hanks 1971). However, we believe the application of the simple models used in this study has outlined in a general way the characteristics of the stress field of island arcs in the north-western Pacific. We now examine this stress field in relation to other indicators of the stress field such as the seismicity and regional tectonics of island arcs in the north-western Pacific.

The Outer Gravity High and the seismicity and regional tectonics of island arcs in the North-Western Pacific

Aleutian Arc

We have noted the Outer Gravity High seaward of the central and eastern Aleutian Trench can be explained by a horizontal compressive stress of the order of a few kilobars acting on the Pacific plate (Fig. 10; Table 2). In the plate tectonic concept the central and eastern Aleutian Trench is presently the location of convergence of the Pacific and North American plates. The large compressive stress field may then be related in a general way to indicators of the stress field along the Aleutian Arc such as seismicity patterns in the vicinity of the arc and the regional tectonics landward of the arc. In addition, since the direction of motion of the Pacific plate relative to the North American plate changes abruptly along the arc we may expect associated changes in the Outer Gravity High seaward of the trench.

Seismic studies can be interpreted as indicating a large compressive stress field presently exists across the central and eastern Aleutian Arcs. Focal mechanism studies of shallow earthquakes (Stauder 1968) in the vicinity of the central and eastern Aleutian Islands can be explained by thrust-faults with NW-SE trending principal axes of compression. In addition, the central and eastern Aleutian Arc is associated with an abundance of shallow earthquakes and large great earthquakes (Kanamori 1971). Important indicators of the size of the large great earthquakes are the length of the rupture zones measured along the arc (Kanamori 1971). The lengths of the rupture zones along the Aleutian Arc are several hundreds of kilometres larger than along other arcs in the western Pacific (Sykes 1971; Kanamori 1971).

Geophysical studies landward of the central and eastern Aleutian Arc indicate the Aleutian and Bowers Basin have been tectonically 'stable' since at least the Early Tertiary. These basins are associated with several kilometres of sediments (Shor 1964), normal heat flow (Foster 1962) and normal P_n velocities (Shor 1964). The

free-air gravity anomalies are nearly zero (Kienle 1971) indicating the basins are presently in isostatic equilibrium. There is a marked contrast between geophysical features of the Aleutian and Bowers Basin and the active inter-arc basins described by Karig (1971a) landward of the Bonin and Mariana Arcs. We conclude there is presently no evidence that an extensional stress field exists landward of the central and eastern Aleutian Arcs. We have not, however, considered the Kamchatka Basin, landward of the western Aleutian Arc. This basin is associated with relatively high heat flow (Foster 1962) and positive gravity anomalies and may be a more recent feature than either the Aleutian or Bowers Basin.

The seismic and tectonic data of the Aleutian Arc are therefore in general agreement with the interpretation of the Outer Gravity High seaward of the trench. We also note that changes in the width and amplitude of the Outer Gravity High correlate in a general way with changes in the relative motion of the Pacific and North American plates. The Outer Gravity High is well developed seaward of the central and eastern Aleutian Trench where the motion of the Pacific plate is nearly normal to the trench and poorly developed seaward of the western Aleutian Trench where the motion is nearly parallel to the trench. It is interesting to note, however, there is still evidence of a regional rise in topography seaward of the western Aleutian Trench.

Kuril and Japan Arcs

The Outer Gravity High seaward of the Kuril and Japan trenches can be explained by a large horizontal compressive stress of the order of a few kilobars applied to the Pacific plate (Hanks 1971; Fig. 10; Table 2). The Outer Gravity High trends parallel to the Kuril and Japan trenches and is approximately perpendicular to the convergence direction deduced by McKenzie & Parker (1967) for the Pacific and Asian plates.

Seismic studies (Barazangi & Dorman 1969; Isacks & Molnar 1971) indicate the Kuril and Japan Arcs are characterized by abundant shallow seismicity, large great earthquakes and deep focus earthquakes extending to about 600 km (Isacks & Molnar 1971).

The sea of Okhotsk and Japan Sea landward of the Kuril and Japan Arcs, are underlain by thin sediments and an oceanic type crust (Korylin, Karts & Shayakhmetov 1966). Heat flow values are relatively high (Vacquier *et al.* 1966) and P_n and S_n velocities are relatively low (Utsu 1971). The low velocity zone may extend from depths of about 80 km to the upper surface of the inclined seismic zone beneath the arcs.

The ages of the Sea of Okhotsk and Japan Sea are not precisely known. It is generally agreed, however, that there has been no active crustal extension in the Japan Sea since the Late Tertiary (Scholz, Barazangi & Sbar 1971). A similar age has been suggested for the Sea of Okhotsk (Karig 1971a).

We can interpret the seismic and tectonic data of the Kuril and Japan Arcs as indicating there is presently a compressive stress field across the arcs which is related to the convergence of the Pacific and Asian plates. This interpretation is in general agreement with the compressive stress field applied to the Pacific plate which is required to explain the Outer Gravity High seaward of the Kuril and Japan Trenches.

Bonin and Mariana Arcs

The width and amplitude of the Outer Gravity High changes significantly seaward of the Bonin and Mariana Trenches. The application of simple flexure models suggests that compressive stresses are required to explain the northern profile of the Bonin Trench but south of about 30° N the profiles can be adequately explained in the absence of compressive stresses (Fig. 10). The change in the width of the Outer

Gravity High at about 30° N does not appear to correlate with any significant changes in the direction of motion of the Pacific Plate.

There are important changes in the seismicity of the Bonin and Mariana Arcs compared to the central and eastern Aleutian, Japan or Kuril Arcs. There is less abundant shallow seismicity (Barazangi & Dorman 1969) and an absence of large great earthquakes. There is also an increase in the steepness of the inclined seismic zone from about 45° for the Japan Arc to about 75° for the southern Bonin Arc. Near 14° N the seismic zone is nearly vertical in the depth range 100 to 400 km (Katsumata & Sykes 1969).

Geological and geophysical evidence (Karig 1971a, b) suggest the narrow basins landward of the Bonin and Mariana Arcs may have formed by active crustal extension. The Mariana Basin is associated with an irregular acoustic basement, thin sediments and relatively high heat flow (Karig 1971b). The presence of active crustal extension is important because it suggests a relief of significant compressive stress field across the arc (Scholz *et al.* 1971).

The seismic and tectonic evidence are therefore in general agreement with the interpretation of the Outer Gravity High seaward of the southern Bonin and Mariana Trenches. We suggest the poorly developed Outer Gravity High seaward of these trenches can be correlated with the presence of active crustal extension landward of the island arc.

Philippine and Ryukyu Arcs

The Outer Gravity High is well developed seaward of the Philippine Trench but cannot be clearly distinguished seaward of the Ryukyu Trench or the Nankai Trough. Computations suggest the Outer Gravity High for the Ryukyu and Philippine Trenches can be explained by large compressive stresses acting on the oceanic plate (Fig. 11).

Seismic studies (Katsumata & Sykes 1969; Fitch 1970; Fitch & Scholz 1971) suggest underthrusting of the Philippine Sea oceanic plate is occurring approximately normal to the Ryukyu and Philippine Trenches. The seismic zone dips steeply beneath the Philippine Islands where earthquakes up to 700 km depth occur. Focal mechanism studies of shallow earthquakes (Katsumata & Sykes 1969) can be explained by thrust-faults with principal axes of compression approximately normal to the trench axis. The seismic zone dips gently beneath the Ryukyu Islands where earthquakes up to about 250 km depth occur.

The presence of a well developed Outer Gravity High seaward of the Philippine Trench raises important questions concerning the tectonics of the Philippine Sea. Wu (1972) has suggested the Philippine Sea behaves as a rigid plate with a motion which can be described about a pole of rotation near the junction of the Bonin Trench and Honshu. For this pole, Wu (1972) suggests the Philippine Sea plate moves clockwise relative to the Asian plate underthrusting the Nankai Trough, Ryukyu and Philippine Trenches at rates which increase southward. Studies of focal mechanism solutions along these arcs cannot, however, be simply explained by a clockwise motion of a single Philippine Sea plate (Katsumata & Sykes 1969). In fact, in order to explain slip vectors for the Ryukyu and Philippine Trenches either a separate plate exists south of Luzon or some other complication is involved (Katsumata & Sykes 1969). The contrast in the width and amplitude of the Outer Gravity High seaward of the Ryukyu and Philippine Trenches also suggests either a separate plate or an additional complication in the tectonics of this region. We point out, however, that correlations for the Aleutian, Kuril and Japan Trenches suggest that the change in the width of the Outer Gravity High is unlikely to correlate with changes in underthrusting rates as implied by the single plate hypothesis of Wu (1972). Rather, the large depth of the Philippine Trench, the steepness of its seaward

wall and the amplitude and width of the Outer Gravity High suggest that the Philippine Trench subduction zone has features similar to those of the Kuril and Japan subduction zones and thus appears to represent the interaction of the Pacific and Asian plates.

We summarize the main features of the correlation of the Outer Gravity High with the seismicity and regional tectonics of the Aleutian, Kuril, Japan, Bonin, Mariana and Philippine Arcs in Table 3.

Table 3

Characteristic features of convergent plate boundaries in the north-western Pacific

Trench system	Marginal basin	Great earthquakes (thrust faults)	Seaward wall of trench	Amplitude of Outer Gravity High
Central and eastern Aleutians	Inactive	Large	Steep	Large
Kuril–Japan–Bonin	Inactive	Large	Steep	Large
Bonin (S)–Mariana	Active	None	Gentle	Small
Philippine	Inactive (?)	Large	Steep	Large

The Outer Gravity High as a general feature seaward of deep-sea trenches

Studies of free air gravity anomaly maps suggest the Outer Gravity High may be a general feature seaward of trenches. We have identified the Outer Gravity High seaward of trenches in the north-eastern Indian, western North Atlantic and southern Pacific oceans. We now briefly describe the Outer Gravity High seaward of four of these trenches.

Java and Sumatra Arcs

The Outer Gravity High is clearly seen in free-air anomaly maps of the Indian Ocean (Talwani & Kahle 1973). The Outer Gravity High extends seaward of the Java and Sumatra Trenches where it reaches widths of about 200 km and amplitudes of about +50 mgal. The northward continuation of the Outer Gravity High is, however, obscured at about 4° N where it merges with positive anomalies associated with the Ninety East Ridge.

Tonga and Kermadec Arcs

Preliminary free-air anomaly maps of the south-western Pacific show an Outer Gravity High seaward of the Tonga and Kermadec Trenches. Unlike the Outer Gravity High seaward of the Java and Sumatra Trenches, however, the Outer Gravity High changes abruptly along these trenches. The Outer Gravity High is poorly developed seaward of the Tonga Trench north of about 24° S. However, the Outer Gravity High is relatively well developed seaward of the Kermadec Trench and its southward continuation, the Hikurangi Trench.

Middle America Arc

Preliminary free-air anomaly maps show a belt of generally positive anomalies seaward of the Middle America Trench. The positive anomalies are, however, interrupted by the gravity effect of irregularities in topography associated with the northward extension of the East Pacific Rise and Cocos Ridge. On some profiles a well-developed regional rise in topography can be distinguished seaward of the trench.

Peru and Chile Arcs

Preliminary studies of extended free-air anomaly profiles across the Peru and Chile Trenches and previously published profiles (Hayes 1966) show a broad belt of positive anomalies occurs seaward of the trenches south of about 18° S. The positive anomalies increase in width from about 300 km for the northern profiles to over 400 km for the southern profiles. These profiles also show a regional rise in the topography seaward of the trench.

The Outer Gravity High correlates in a general way with the seismicity and regional tectonics of these arcs. The Outer Gravity High is well developed seaward of the Java and Sumatra, Peru and Chile and Middle America Arcs. These arcs are associated with abundant shallow seismicity and an absence of an active inter-arc basin landward of the arc. The Tonga Arc, however, is associated with abundant shallow seismicity and an active inter-arc basin landward of the arc.

We have not, however, made a detailed quantitative study of the stress field required to explain the Outer Gravity High for these arcs. We plan to make this study when free-air gravity maps for these arcs are completed.

The Outer Gravity High, satellite derived gravity anomalies across island arcs and the gravity effect of the downgoing lithospheric slab

A satellite derived gravity anomaly map of the north-western Pacific obtained from the combination solution of Gaposchkin & Lambeck (1971) to the 16th degree and order is shown in Fig. 12. The map shows circular positive gravity anomalies of about +20 mgal amplitude associated with the eastern Aleutian, Mariana and Bonin Arcs. There are significant gaps in the positive anomalies for the central parts of the Kuril and central Aleutian Arcs. The gravity anomaly highs associated with island arcs on satellite derived maps have been correlated in a general way with the gravity effect of a cool downgoing lithospheric slab (Kaula 1972). However, no attempts have been made to quantitatively relate the gravity highs to downgoing slabs.

Attempts have been made, however, to quantitatively relate surface gravity measurements across island arcs and trenches to the gravity effect of a downgoing slab (Hatherton 1969, 1970; Griggs 1972).

Griggs (1972) compared an observed free-air anomaly profile of the Tonga Arc to a computed profile representing the gravity effect of the topography, the downgoing slab and a form of regional compensation for the slab and trench. In the computations he did not use the actual topography but considered the topography to be represented by a trench symmetrical about its axis. He thus ignored the topography of the Tonga Arc. Free-air anomaly profiles across the Tonga Arc (Talwani, Worzel & Ewing 1961) show, however, a good correlation between the maximum free air anomaly and the crest of the Tonga Ridge. It would therefore appear likely that the maximum free-air anomaly is related most closely with the topographic and structural effect of the Tonga Ridge and it would be incorrect to suggest it was caused completely by the gravity effect of a downgoing slab and its compensation. We also note that the computed effect for Griggs (1972) best-fitting model integrates to zero over a distance slightly greater than 1000 km. Thus the computed effect of Griggs (1972) could not give rise to the long wavelength gravity anomalies in island arc regions deduced from observations of satellites.

Hatherton (1969 & 1970) considered topography in his computations by using isostatic anomalies based on the Airy-Heiskanen hypothesis of isostasy. He interpreted the isostatic anomalies as caused by density variations in the upper mantle. He therefore implied that the Airy-Heiskanen hypothesis of isostasy was generally correct at island arcs and that the isostatic anomalies were caused by a relatively deep

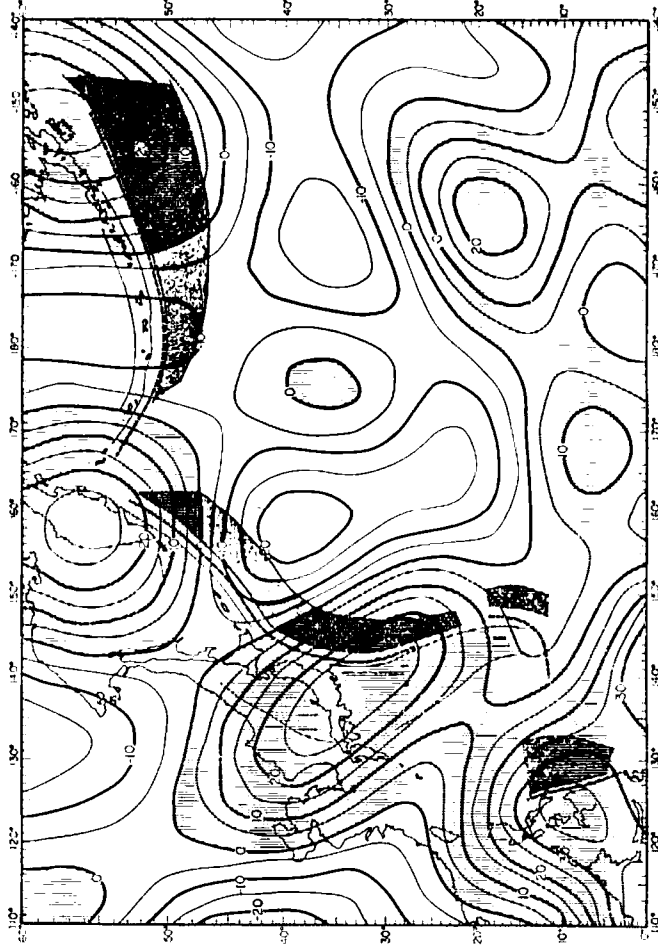


Fig. 12. Gravity map of the north-western Pacific derived from the combination solution of Gaposchkin & Lambeck (1971). The gravity map and the Inner and Outer Gravity Highs (Fig. 1) have been referred to the equilibrium figure of the Earth.

mass distribution. Enough is known, however, about the shallow and deep structure of island arcs to suggest that the assumption of Airy-Heiskanen isostasy is quite invalid. Therefore at least part of the isostatic anomalies must be due to mass distributions at relatively shallow depths not predicted by the Airy-Heiskanen hypothesis of isostasy.

In this paper we have shown there is a close correlation between the Outer Gravity High and a regional rise in topography seaward of trenches. The Outer Gravity High can most satisfactorily be explained by simple models of flexure of the oceanic lithosphere seaward of trenches. Because of the close correlation between the Outer Gravity High and the topography seaward of trenches we consider the gravity effect of a downgoing slab is likely to be small and confined in lateral extent to the region of the island arc and trench. Undoubtedly the gravity effect of the dense downgoing slab contributes to the gravity field of island arcs. However, we feel this contribution is small and is unlikely to fully explain the gravity anomaly highs on satellite derived maps or the local gravity highs on surface ship measurements.

If the gravity effect of the downgoing slab is small as shown for the Aleutian arc in Fig. 7 we do not consider it is possible, in the presence of much larger anomalies associated with the trench and the island arc, to obtain details of the configuration and density distribution of a downgoing slab directly from observed surface measurements.

There is still the question of the cause of the satellite derived gravity highs associated with island arcs. We have suggested above that the gravity effect of the dense downgoing slab is too small. We can also see that the simple models of flexure of the oceanic lithosphere considered in this study will not produce a net gravity high since

the total gravity effect associated with the deflection of the oceanic lithosphere must integrate to zero. Our model profiles in Fig. 9 appear to show a total negative gravity effect. However, if the applied forces had been replaced by an equivalent load and if profiles had been integrated over sufficient distances on either side of the trench the integral would be zero.

We have noted that surface gravity maps show near zero gravity values landward of the Aleutian arc but largely positive values landward of the Bonin and Mariana arc. This suggests the possibility that the satellite derived highs associated with island arcs correlate most closely with those areas in which evidence indicates active crustal extension occurs landward of arcs.

However, any attempts to explain the satellite derived field are further complicated because this field only represents long-wavelength information of the Earth's gravity field. This is shown (Fig. 12) by the contrast in extent of the gravity highs obtained by surface ship and satellite data. Clearly we need to obtain more short-wavelength data in the area behind arcs to examine more carefully the correlation between gravity highs and extensional basins and then to seek causes for this correlation.

Acknowledgments

We are grateful to Tom Hanks, Klaus Jacob, Chris Scholz and Lynn Sykes for critically reading the manuscript and for helpful suggestions. Discussions with Jim Cochran and Dick Bischke have also been useful. This study was supported by National Science Foundation Grants GV-27472, GA-27281, GA-17761, GA-1434, GA-1523 and by the Office of Naval Research Contract N00014-67-A-0108-0004. The acquisition of the large amount of data in this study would not have been possible without the foresight of Maurice Ewing who initiated and led Lamont-Doherty's geophysical surveys in the world oceans and without the help of the officers, gravity observers and scientists aboard the research vessels *Vema* and *Robert D. Conrad*.

*Lamont-Doherty Geological Observatory,
Palisades, New York 10964*

References

- Abe, K., 1972. Lithospheric normal faulting beneath the Aleutian trench, *Physics Earth Planet. Int.*, **5**, 190.
- Barazangi, M. & Dorman, J., 1969. World seismicity maps compiled from ESSA. Coast and Geodetic Survey, epicenter data, 1961-1967, *Bull. seism. Soc. Am.*, **59**, 369.
- Barnes, D. F., 1969. Progress on a gravity map of Alaska, EOS, *Trans. Am. geophys. Un.*, **50**, 550.
- Carr, W. J., Gard, I. M., Bath, G. D. & Healey, D. L., 1971. Earth Science studies of a nuclear test area in the western Aleutian islands, Alaska: An interim summary, *Bull. geol. Soc. Am.*, **82**, 699.
- Chase, T. E., Menard, H. W. & Mammerickx, J., 1970. *Bathymetry of the North Pacific*, Scripps Institution of Oceanography and Institute of Marine Resources, Chart numbers 1, 2, 3, 5, 6, and 7.
- Dickinson, W. R., 1972. Evidence for plate-tectonic regimes in the rock record. *Am. J. Science*, **272**, 551.
- Elsasser, W. M., 1971. Sea-floor spreading as thermal convection, *J. geophys. Res.*, **76**, 1101.
- Fisher, R. L. & Hess, H. H., 1965. Trenches, *The Sea*, Volume 3, p. 411, John Wiley & Sons, New York.
- Fitch, T. J., 1970. Earthquake mechanisms and island arc tectonics in the Indonesian-Philippine region. *Bull. seism. Soc. Am.*, **60**, 565.

- Fitch, T. J. & Scholz, C. H., 1971. Mechanism of underthrusting in southwest Japan: A model of convergent plate interactions, *J. geophys. Res.*, **76**, 7260.
- Foster, T. D., 1962. Heat-flow measurements in the northeast Pacific and in the Bering Sea, *J. geophys. Res.*, **67**, 2991.
- Gainanov, A. G., 1955. Pendulum determinations of gravity in the Northwest Pacific Ocean, *Tr. International Okeanol. AN SSR*, **12**, 145 (in Russian).
- Gaposchkin, E. M. & Lambeck, K., 1971. Earth's gravity field to the sixteenth degree and station coordinates from satellite and terrestrial data, *J. geophys. Res.*, **76**, 4855.
- Graf, A. & Schulze, R., 1961. Improvements on the sea gravimeter Gss2, *J. geophys. Res.*, **66**, 1813.
- Griggs, D., 1972. The sinking lithosphere and the focal mechanism of deep earthquakes, *The nature of the solid Earth*, p. 361, McGraw-Hill, New York.
- Gunn, R., 1943. A quantitative evaluation of the influence of the lithosphere on the anomalies of gravity, *J. Franklin Inst.*, **236**, 373.
- Hanks, T. C., 1971. The Kuril trench-Hokkaido rise system: Large shallow earthquakes and simple models of deformation, *Geophys. J. R. astr. Soc.*, **23**, 173.
- Hasebe, K., Fujii, N. & Uyeda, S., 1970. Thermal processes under island arcs, *Tectonophysics*, **10**, 335.
- Hatherton, T., 1969. Gravity and seismicity of asymmetric active regions. *Nature, Lond.*, **221**, 353.
- Hatherton, T., 1970. Upper mantle beneath New Zealand: Surface Manifestations. *J. geophys. Res.*, **75**, 269.
- Hayes, D. E., 1966. A geophysical investigation of the Peru-Chile trench, *Marine Geology*, **4**, 309.
- Hayes, D. E. & Ewing, M., 1970. Pacific boundary structure, *The Sea*, Volume 4, p. 29, New York, John Wiley & Sons.
- Hayes, D. E., Worzel, J. L. & Karnick, H., 1964. Tests on the 1962 model of the Anschutz gyrotable, *J. geophys. Res.*, **69**, 749.
- Hetényi, M., 1946. *Beams on elastic foundation*, The University of Michigan Press, Ann Arbor, Michigan.
- Hilde, T. W. C., Wageman, J. M. & Hammond, W. T., 1969. The structure of Tosa terrace and Nankai trough off southeastern Japan, *Deep Sea Res.*, **16**, 67.
- Isacks, B. & Molnar, P., 1971. Distribution of stresses in the descending lithosphere from a global survey of focal-mechanism solutions of mantle earthquakes, *Rev. Geophys.*, **9**, 103.
- Jacob, K. H., 1972. Global tectonic implications of anomalous seismic P travel times from the nuclear explosion Longshot, *J. geophys. Res.*, **77**, 2556.
- Jacoby, W. R., 1970. Instability in the upper mantle and global plate movements, *J. geophys. Res.*, **75**, 5671.
- Jones, E. J. W., Ewing, J. & Truchan, M., 1971. Aleutian plain sediments and lithospheric plate motions, *J. geophys. Res.*, **76**, 8121.
- Kanamori, H., 1971. Great earthquakes at island arcs and the lithosphere, *Tectonophysics*, **12**, 187.
- Karig, D. E., 1971a. Origin and development of marginal basins in the western Pacific, *J. geophys. Res.*, **76**, 2543.
- Karig, D. E., 1971b. Structural history of the Marianas island arc system, *Bull. geol. Soc. Am.*, **82**, 323.
- Katsumata, M., & Sykes, L. R., 1969. Seismicity and tectonics of the western Pacific: Izu-Mariana-Caroline and Ryukyu-Taiwan regions, *J. geophys. Res.*, **74**, 5923.
- Kaula, W. M., 1972. Global gravity and mantle convection. *Tectonophysics*, **13**, 341.
- Kienle, J., 1971. Gravity and magnetic measurements over Bowers Ridge and Shirshov Ridge, Bering Sea, *J. geophys. Res.*, **76**, 7138.

- Kovylin, V. M. Karts, B. Y. & Shayakhmetov, R. B., 1966. Structure of the crust and sedimentary layer of the sea of Japan based on seismic data, *Doklady Akad. Nauk SSSR*, **168**, 1048.
- La Coste, L. J. B. & Harrison, J. C., 1961. Some theoretical considerations in the measurement of gravity at sea, *Geophys. J. R. astr. Soc.*, **5**, 89.
- Le Pichon, X., 1968. Sea-floor spreading and continental drift, *J. geophys. Res.*, **73**, 3661.
- Lliboutry, L., 1969. Sea-floor spreading, continental drift and lithosphere sinking with anasthenosphere at melting point, *J. geophys. Res.*, **74**, 6525.
- Ludwig, W. J., Ewing, J. I., Ewing, M., Murauchi, S., Den, N., Asano, S., Hotta, H., Hayakawa, M., Asanuma, T., Ichikawa, K. & Noguchi, I., 1966. Sediments and structure of the Japan trench, *J. geophys. Res.*, **71**, 2121.
- Malahoff, A. & Erickson, B. H., 1969. Gravity anomalies over the Aleutian trench, *EOS, Trans. Am. geophys. Un.*, **50**, 552.
- Mammerickx, J., 1970. Morphology of the Aleutian abyssal plain, *Bull. geol. Soc. Am.*, **81**, 3457.
- McKenzie, D. P. & Parker, R. L., 1967. The North Pacific: An example of tectonics on a sphere, *Nature, Lond.*, **216**, 1276.
- Menard, H. W., 1964. *Marine geology of the Pacific*, McGraw-Hill.
- Minear, J. W. & Toksöz, M. N., 1970. Thermal regime of a downgoing slab and new global tectonics, *J. geophys. Res.*, **75**, 1397.
- Oliver, J. & Isacks, B., 1967. Deep earthquake zones, anomalous structures in the upper mantle, and the lithosphere, *J. geophys. Res.*, **72**, 4259.
- Oxburgh, E. R. & Turcotte, D. L., 1970. Thermal structure of island arcs, *Bull. geol. Soc. Am.*, **81**, 1665.
- Peter, G., Elvers, D. & Yellin, M., 1965. Geological structure of the Aleutian trench southwest of Kodiak Island, *J. geophys. Res.*, **70**, 353.
- Press, F. S. & Kanamori, H., 1970. How thick is the lithosphere? *Nature, Lond.*, **226**, 330.
- Scholz, C. H., Barazangi, M. & Sbar, M. L., 1971. Late Cenozoic Evolution of the Great Basin, Western United States, as an ensialic interarc basin, *Bull. geol. Soc. Am.*, **82**, 2979.
- Schubert, G. & Turcotte, D. L., 1972. One-dimensional model of shallow mantle convection, *J. geophys. Res.*, **77**, 945.
- Segawa, J., 1970. Gravity measurements at sea by use of the T.S.S.G. Part 2. Results of the measurements, *J. Phys. Earth*, **18**, 203.
- Shimazaki, K., 1972. Focal mechanism of a shock at the northwestern boundary of the Pacific Plate: Extensional feature of the oceanic lithosphere and compressional feature of the continental lithosphere, *Phys. Earth Planet. Ints.*, **6**, 397.
- Shor, G. G., 1964. Structure of the Bering Sea and the Aleutian Ridge, *Marine Geology*, **1**, 213.
- Sleep, N. & Toksöz, M. N., 1971. Evolution of marginal basins, *Nature, Lond.*, **233**, 548.
- Stauder, W., 1968. Tensional character of earthquake foci beneath the Aleutian trench with relation to sea-floor spreading, *J. geophys. Res.*, **73**, 7693.
- Sykes, L. R., 1971. Aftershock zones of great earthquakes, seismicity gaps and earthquake prediction for Alaska and the Aleutians, *J. geophys. Res.*, **76**, 8021.
- Talwani, M., 1970. Gravity, *The Sea*, **4**, 251, New York, John Wiley & Sons.
- Talwani, M. & Kahle, H. -G., 1973. Free air gravity charts of the Indian Ocean, *The Atlas of Geology and Geophysics of the International Indian Ocean Expedition*, Chief editor: G. Udintsev, in press.
- Talwani, M., Sutton, G. M. & Worzel, J. L., 1959. A crustal section across the Puerto Rico trench, *J. geophys. Res.*, **64**, 1545.

- Talwani, M., Worzel, J. L. & Ewing, M., 1961. Gravity anomalies and crustal section across the Tonga trench, *J. geophys. Res.*, **66**, 1265.
- Tomoda, Y. & Kanamori, H., 1962. Tokyo surface-ship gravity meter $\alpha-1$. *Collected reprints, Ocean Res. Inst. Univ. Tokyo*, **1**, 116.
- Tomoda, Y., Segawa, J. & Tokohiro, A., 1970. Free-air gravity anomalies at sea around Japan measured by the Tokyo Surface Ship Gravity meter (1961-69), *Proc. Japan Acad.*, **46**, 1006.
- U.S. Dept. of Commerce, 1964. International Indian Ocean Expedition. *USC & GS ship PIONEER—1964*, **1**, 139p.
- Utsu, T., 1971. Seismological evidence for anomalous structure of island arcs with special reference to the Japanese region, *Rev. Geophys.*, **9**, 839.
- Vacquier, V., Uyeda, S., Yasui, M., Slater, J., Corry, C. & Watanabe, T., 1966. Heat-flow measurements in the north western Pacific, *Bull. earthq. Rep., Inst. Toyko Univ.*, **44**, 1519.
- Vening Meinesz, F. A., 1948. *Gravity expeditions at sea, 1923-1938*. Neth. Geod. Comm., Waltman, Delft.
- Vening Meinesz, F. A., 1964. *The Earth's crust and mantle*, Elsevier Publishing Co.
- Walcott, R. I., 1970. Flexural rigidity, thickness, and viscosity of the lithosphere, *J. geophys. Res.*, **75**, 3941.
- Woollard, G. P. & Rose, J. C., 1963. *International gravity measurements*. Society of Exploration Geophysicists, Tulsa, Oklahoma.
- Worzel, J. L., 1965. *Pendulum gravity measurements at sea 1936-1959*, John Wiley, New York.
- Wu, F. T., 1972. The Philippine sea plate: A "sinking towel"?, *Tectonophysics*, **14**, 81.